INTERGENERATIONAL REDISTRIBUTION IN THE GREEN TRANSITION

BARBARA ANNICCHIARICO JEAN-GUILLAUME SAHUC GAUTHIER VERMANDEL

ABSTRACT. We study the intergenerational distributional effects of carbon pricing during the green transition in an overlapping-generations New Keynesian model calibrated to euro-area household micro data. Climate policy generates systematic redistribution across cohorts through two channels: a *labor-income channel*, driven by wage compression and lower labor demand, and a *financial-wealth channel*, driven by asset revaluation and higher real returns. The labor-income channel dominates quantitatively, generating persistent welfare losses of up to 6 percent in permanent-consumption equivalents for working-age households, while retirees experience comparable gains. Revenue recycling can mitigate these asymmetries, requiring 40 to 68 percent of carbon-tax revenues to be directed toward financial-income tax relief. Monetary policy has limited influence on the overall redistributive pattern.

JEL: E21, E32, E52, H23, Q54.

Keywords: Climate policy, carbon pricing, intergenerational redistribution, overlapping generations, fiscal policy, New Keynesian model

1. INTRODUCTION

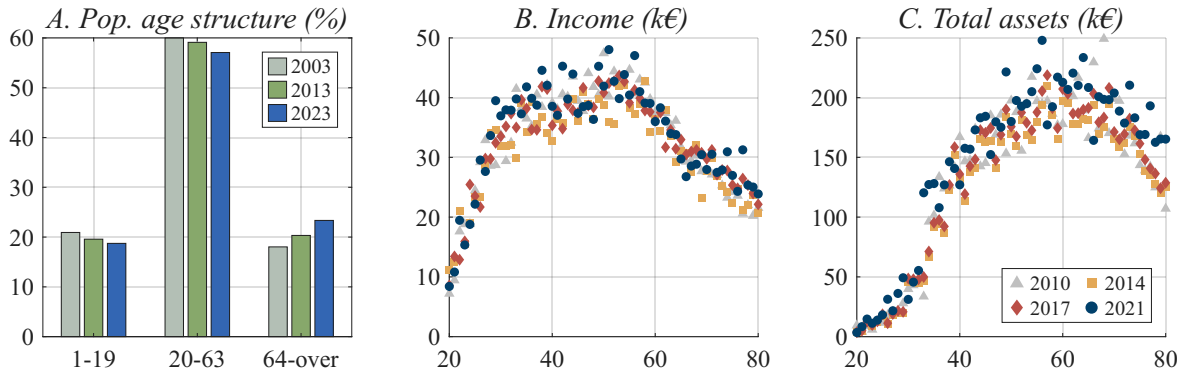
Carbon pricing is often presented as a generation-neutral instrument: it corrects a market failure, raises revenues, and, if properly recycled, can improve aggregate welfare. This paper argues that this view is incomplete. In an overlapping-generations (OLG) economy with heterogeneous income sources, carbon tax reforms generate systematic redistribution across cohorts. The mechanism is rooted in a structural life-cycle asymmetry. Working-age households rely primarily on labor income, whereas retirees rely more heavily on accumulated financial wealth. Carbon pricing affects these income sources in opposite directions. By raising production costs, it compresses wages and disproportionately affects households dependent on labor income (*labor-income channel*). At the same time, the transition-induced

May 2026. B. Annicchiarico: Roma Tre University, Via Ostiense, 163–00154 Roma, Italy (e-mail: barbara.annicchiarico@uniroma3.it); J.-G. Sahuc: Banque de France, 31 rue Croix des Petits Champs, 75049 Paris, France, and University Paris-Nanterre (e-mail: jean-guillaume.sahuc@banque-france.fr); G. Vermandel: Ecole Polytechnique, CMAP UMR CNRS 7641, Route de Saclay, Palaiseau and University Paris-Dauphine, LEDA UMR CNRS 8007, Place du Maréchal de Lattre de Tassigny, 75016 Paris, France (e-mail: gauthier@vermandel.fr).
We thank Marcin Bielecki, Rebecca Clipal, Janusz Jablonowski, and Marcin Kolasa for their help and/or comments. The views expressed in this paper are those of the authors and do not necessarily reflect the views of the Banque de France or the Eurosystem. Gauthier Vermandel thanks the Stress-test chair for financial support. Declarations of interest: none.

decline in aggregate demand dampens inflation, raises the real value of nominal assets, and increases real financial returns (*financial-wealth channel*). Since reliance on labor income declines steadily with age, from almost one for young workers to nearly zero for retirees, these opposing effects generate a systematic transfer from workers to retirees. We call this the *redistribution force* of climate policy.

We quantify this force for the euro area, where both ingredients are pronounced. As shown in Figure 1, the population is aging rapidly, amplifying the demographic footprint of any generational transfer (Panel A), and cross-cohort differences in income composition and total asset holdings are large (Panels B and C). Climate policy is persistent and ambitious: as signatories to the Paris Agreement, euro-area countries have committed to a sustained carbon price path consistent with limiting warming to below 2°C. These structural features imply that the green transition generates redistribution that is not incidental to carbon pricing but inherent to it.

FIGURE 1. Population structure and household balance sheets in the euro area



Note: This figure reports the population age structure by major age groups as a share of total population (Panel A), median before-tax income (Panel B), and total assets (Panel C) by single year of age for households aged 20 to 80. Data are drawn from the United Nations World Population Prospects (United Nations, 2024) and four waves of the Household Finance and Consumption Survey (HFCN, 2023).

To this end, we build an *environmental overlapping-generations New Keynesian model* calibrated to euro-area micro data. Cohorts differ in labor income profiles, asset holdings, and mortality risk in a way disciplined by four waves of the Household Finance and Consumption Survey (HFCS) and United Nations Life Tables. The model is solved under perfect foresight along transition paths, thereby capturing the nonlinear dynamics induced by climate policy. We condition on two externally disciplined carbon pricing paths from Barrage and Nordhaus (2024): the *Paris Agreement*, consistent with limiting warming to below 2°C, and *Low Carbon Price*, which extrapolates current policies with a global average carbon price of

\$6/tCO$_2$ growing at 2.5% annually. Rather than solving for an optimal tax, we characterize how these predetermined trajectories transmit through the euro-area economy and generate distinct welfare dynamics across cohorts.

Three findings emerge from our analysis. First, the *labor-income channel* dominates. First, the labor-income channel dominates. Aggregate labor income falls by nearly 10 percent over the first three decades of the transition, while the offsetting gains from the financial-wealth channel are smaller in magnitude and short-lived, fading as inflation expectations adjust. In consumption-equivalent terms, working-age cohorts incur welfare losses of up to 6 percent of permanent consumption, while retirees gain up to 6 percent. This dominance is amplified by three structural features of the euro area: the short-run asymmetric incidence of abatement costs on wages, portfolio adjustment frictions that limit self-insurance, and a life-cycle gradient in marginal propensities to consume consistent with the HFCS microdata. Crucially, the welfare costs are not transitory. Cohorts exposed to wage compression during their peak earning years save less, enter retirement with a depleted wealth base, and bear losses for the remainder of their lives. This scarring mechanism outlasts the physical transition by more than two decades, reflecting the slow-moving dynamics of wealth accumulation.

Second, fiscal policy is the main instrument shaping the intergenerational incidence of carbon pricing. Recycling carbon revenues through labor tax cuts directly weakens the labor-income channel, reducing the welfare burden on working-age households and lowering consumption inequality across cohorts. Retirees, however, are mechanically disadvantaged by this canonical double-dividend design. Relative to lump-sum transfers, labor-tax recycling reallocates carbon revenues toward workers and away from retirees, who would otherwise benefit from uniform rebates. By contrast, recycling through financial-income tax cuts strengthens the financial-wealth channel, compensates retirees, and improves aggregate efficiency, but at the cost of greater consumption inequality. Neither instrument alone achieves both objectives across all recycling intensities. Nevertheless, a feasible policy window emerges: allocating between 40 and 68 percent of carbon revenues to financial-income tax relief simultaneously compensates retirees and limits inequality, defining a corridor of equitable and efficient policy design.

Third, monetary policy has only limited capacity to alter the redistribution generated by the transition. This result reflects two complementary factors. Carbon pricing operates through real forces, changes in production costs and factor returns, so nominal rigidities do

not drive the main redistributive effects. The OLG structure further weakens the standard intertemporal substitution channel: declining survival probabilities shorten households' effective planning horizons, dampening their consumption response to interest-rate changes and attenuating the transmission from policy rates to labor supply, wages, and labor income. As a result, the distributional consequences of the transition remain broadly unchanged across monetary policy regimes.

This paper contributes to three strands of literature on climate policy, monetary economics, and heterogeneous-agent macroeconomics. First, we contribute to the literature on the intergenerational incidence of climate policy in overlapping-generations economies (Karp and Rezai, 2014; Kotlikoff et al., 2021, 2024; Fried et al., 2024; Kuhn and Schlattmann, 2024; Rezai and van der Ploeg, 2026). Recent work has incorporated some of the ingredients we study, including heterogeneous-household climate models with nominal rigidities and overlapping-generations analyses of carbon-pricing incidence. Our contribution is to combine these elements in an environmental OLG New Keynesian model calibrated to euro-area micro data, and to decompose the transition into two distinct mechanisms: a labor-income channel operating through wage compression, and a financial-wealth channel operating through asset revaluation and higher real returns. Solving the model along the full transition path allows us to trace how these channels generate persistent intergenerational redistribution, beyond what steady-state comparisons can capture.[1]

Second, we relate to the literature on redistribution through monetary policy in heterogeneous-household models and life-cycle economies (Auclert, 2019; Kaplan and Violante, 2014; Lis et al., 2020; Bielecki et al., 2022, 2023). This literature shows that inflation and interest-rate movements have heterogeneous welfare effects because households differ systematically in portfolio composition and marginal propensities to consume over the life cycle. We extend this perspective to the context of climate transitions. Rather than focusing on redistribution generated by cyclical demand disturbances or monetary shocks, we study a persistent decarbonization process that unfolds through gradual adjustments in wages, inflation, and asset returns over several decades. This framework allows us to evaluate whether conventional monetary stabilization policy can materially alter the intergenerational redistribution induced by climate policy.

[1] The intergenerational implications of environmental taxation have been studied since the double dividend debate. Building on Baumol and Oates (1988), overlapping-generations frameworks (John and Pecchenino, 1994; Bovenberg and Heijdra, 1998) established that environmental taxation is generally not welfare neutral across cohorts.

Third, our paper speaks to the literature on heterogeneous-agent climate policy (Benmir and Roman, 2022; Douenne et al., 2026) by emphasizing demographic heterogeneity as a central propagation mechanism of the transition. In our framework, differences in labor income exposure, wealth accumulation, and mortality risk emerge endogenously over the life cycle rather than solely from idiosyncratic earnings risk. By disciplining these dimensions with household survey and demographic data, we provide an empirically grounded quantification of intergenerational redistribution in one of the world's largest carbon-pricing jurisdictions. This approach also allows us to characterize how alternative carbon-revenue recycling schemes trace out an intergenerational policy frontier between efficiency and equity over the full transition path.

The remainder of the paper is organized as follows. Section 2 introduces the model. Section 3 describes the calibration and data. Section 4 analyzes aggregate transition dynamics under alternative carbon pricing paths. Section 5 quantifies the intergenerational redistribution dynamics. Section 6 studies the role of fiscal policy and carbon revenue recycling. Section 7 examines the role of monetary policy. Section 8 concludes.

2. An environmental New Keynesian model with overlapping generations

The economy is described by an environmental New Keynesian model with overlapping generations of finitely lived households. Households enter the model when they start working at a real-world age of 20 (index $j = 1$), live for a maximum of 99 years ($J = 80$) and survive each period (a year) with an age-specific probability ω_j (Bielecki et al., 2022, 2023). They work until the retirement age of 64 ($JR = 45$). As a result, the economy is populated by 80 overlapping cohorts of varying size in each period. Households maximize intertemporal utility by choosing consumption, labor supply, and financial asset holdings. On the production side, perfectly competitive final-good firms combine differentiated intermediate goods produced by monopolistically competitive firms that face Rotemberg price adjustment costs. Investment funds intermediate household savings into portfolios of physical capital and bonds and rent capital services to intermediate-good producers. Production generates CO_2 emissions, whose accumulated stock affects productivity and therefore alters production possibilities (Golosov et al., 2014). Firms do not internalize the environmental damages associated with their emissions, which motivates the implementation of a carbon tax by the government. Firms can partially reduce emissions through costly abatement activities (Heutel, 2012; Annicchiarico and Di Dio, 2015; Jondeau et al., 2026). The economy is further characterized by monetary and fiscal authorities conducting stabilization and redistribution policies. Finally,

the model incorporates four exogenous long-run trends (population dynamics, carbon intensity, abatement efficiency, and technological progress) to capture the structural evolution of the economy and emissions during the transition. Accounting for these structural trends is important in macro-climate models because they shape long-run emissions trajectories, climate outcomes, and therefore equilibrium expectations during the transition.

2.1. **Household sector.**

2.1.1. *Households' preferences.* Let $N_{j,t}$ denote the mass of households of the generation j alive at time t. The representative household of the generation j derives utility from consumption, $c_{j,t}$, and disutility from labor $h_{j,t}$. The expected lifetime utility function is of the form:

$$\mathcal{U}_{j,t} = \mathbb{E}_t \left\{ \sum_{s=0}^{J-j} \beta^s \frac{N_{j+s,t+s}}{N_{j,t}} \left(\log c_{j+s,t+s} - \varphi_{j+s} \frac{h_{j+s,t+s}^{1+\nu}}{1+\nu} \right) \right\}, \tag{1}$$

where $\mathbb{E}_t$ denotes the mathematical expectation operator conditional upon information available at t, $\beta \in (0,1)$ is the constant discount factor, the ratio $N_{j+s,t+s}/N_{j,t}$ measures the probability of staying alive in other s years, φ_{j+s} is an age-dependent scale coefficient that measures the disutility of labor and $\nu > 0$ is the inverse of the Frisch labor supply elasticity. Households work only until retirement age JR: for $j \geq JR$ we set $h_{j,t} = 0$, so retirees derive utility from consumption alone.

The period-by-period budget constraint of the typical household j reads as

$$\begin{aligned} P_t(c_{j,t} + a_{j+1,t+1} + \mathcal{C}^x_{j,t}) = {} & (1-\tau_h)\mathcal{I}_{j<JR} W_t z_j h_{j,t} \\ & + (1-\tau_a)(R^a_t - 1)P_{t-1}a_{j,t} + P_{t-1}a_{j,t} + P_t beq_t + P_t \tau_{j,t}, \end{aligned} \tag{2}$$

where P_t is the price index and $a_{j,t}$ denotes the real stock of financial wealth carried over from the previous period.[2] Financial wealth yields a nominal gross return R^a_t (where τ_a is the tax rate on financial income), τ_h is the tax rate on labor income, $\mathcal{I}_{j<JR}$ is an indicator variable that equals 1 if the household is of working age, W_t is the nominal wage and z_j measures an age-dependent labor productivity level. In addition, two boundary conditions close the household's problem. First, members of the youngest generation enter adulthood with no financial assets, that is $a_{1,t} = 0$. Second, as agents do not survive beyond age J, they consume all remaining wealth in their final period of life, implying $a_{J+1,t+1} = 0$. However, since most

[2]The notation $a_{j+1,t+1}$ reflects the timing convention of the model: it denotes the financial wealth accumulated by a generation-j household during period t, which becomes available in period $t+1$, when that household transitions to age $j+1$. Thus, assets carried into period $t+1$ are indexed by the next-period age and the next-period date.

agents pass away before reaching their maximum life expectancy, they leave unintentional bequests of financial wealth that are confiscated by the fiscal authority and then redistributed equitably among all surviving agents through lump-sum transfers, denoted beq_t. The term $\tau_{j,t}$ is a catch-all variable that includes all net transfers made by the fiscal authority. Together, these elements determine the household's net cash flow,

$$x_{j,t} = (1 - \tau_h)\mathcal{I}_{j<JR}\frac{W_t}{P_t}z_j h_{j,t} + beq_t + \tau_{j,t} - c_{j,t}, \tag{3}$$

which is the residual that accumulates into financial wealth. Rebalancing wealth is not frictionless: the household pays a quadratic cost on the size of this flow,

$$\mathcal{C}^x_{j,t} = \frac{\kappa_{x,t}}{2}\, x^2_{j,t}, \qquad \kappa_{x,t} > 0. \tag{4}$$

The friction makes any deviation from a hand-to-mouth allocation costly, and is meant to capture the degree of illiquidity of financial wealth.[3] The friction binds in steady state as well as along transitions: working-age cohorts pay a non-zero cost on the saving needed to fund retirement, and retirees pay a cost on dissaving.

Finally, as in Huggett (1996), households face a no-borrowing constraint:

$$a_{j,t} \geq 0 \quad \text{for all } j \text{ and } t. \tag{5}$$

This constraint is the key ingredient that generates a realistic life-cycle profile of marginal propensities to consume, in line with the empirical evidence in Christelis et al. (2019). Without it, young households would smooth transitory income shocks by borrowing against future earnings, producing a counterfactually low marginal propensity to consume at the start of the life cycle.[4]

2.1.2. *Demographics and aggregation.* The demographic structure is determined by the growth rate of the youngest generation, $n = N_{1,t+1}/N_{1,t} - 1$, assumed exogenous and constant, and by the age-dependent mortality risk ω_j, assumed time-invariant. The total number of agents

[3] In the spirit of Kaplan and Violante (2014), the adjustment cost limits households' ability to re-balance their asset positions and hence to smooth consumption, raising the marginal propensity to consume out of transitory income fluctuations. To preserve stationarity when the model is expressed in efficiency units, the parameter governing the size of this cost scales with trend productivity, Z_t: $\kappa_{x,t} = \kappa_x / Z_t$, where $\kappa_x > 0$.

[4] This is the case, for instance, in Bielecki et al. (2022), who abstract from a borrowing limit, which tends to make the youngest cohorts exhibit very low (close to zero) marginal propensities to consume, at odds with the data. In our context, this friction is crucial: young households are less able to smooth the (transition) costs induced by climate policies, so the green transition can generate stronger intergenerational asymmetries.

alive at time t is thus given by

$$N_t = \sum_{j=1}^{J} N_{j,t}, \tag{6}$$

where the mass of agents in each cohort $j > 1$ evolves over time as follows

$$N_{j+1,t+1} = (1 - \omega_j) N_{j,t}. \tag{7}$$

We assume the economy starts in the demographic steady state, so that total population grows at the constant rate n while the absolute size of each cohort grows over time. We therefore work with relative cohort sizes,

$$N_j^{rel} = \frac{N_{j,t}}{N_t}, \tag{8}$$

which are time-invariant given our assumptions on n and ω_j. Equation (7) can then be rewritten in stationary form as

$$N_{j+1}^{rel} = \frac{1 - \omega_j}{1 + n} N_j^{rel}. \tag{9}$$

Asset markets clear at the end of period t, before period-$(t+1)$ mortality is realized. Aggregate wealth carried into $t+1$ therefore includes the assets of cohorts that will not survive; their balances are redistributed in the following period through the bequest term beq_{t+1}. The aggregate allocations over all existing households can then be represented in per capita terms as follows:

$$c_t = \sum_{j=1}^{J} N_j^{rel} c_{j,t}, \tag{10}$$

$$h_t = \sum_{j=1}^{JR-1} N_j^{rel} z_j h_{j,t}, \tag{11}$$

$$a_{t+1} = \sum_{j=1}^{J-1} \frac{N_j^{rel}}{1 + n} a_{j+1,t+1}, \tag{12}$$

$$\mathcal{C}_t^x = \frac{\kappa_{x,t}}{2} \sum_{j=1}^{J} N_j^{rel} x_{j,t}^2, \tag{13}$$

$$\tau_t = \sum_{j=1}^{J} N_j^{rel} \tau_{j,t}. \tag{14}$$

Finally, the unintentional bequests left by deceased agents rebated to surviving households are given by

$$beq_t = \sum_{j=2}^{J} \frac{\omega_{j-1} N_{j-1}^{rel}}{1 + n} \frac{[1 + (1 - \tau_a)(R_t^a - 1)] a_{j,t}}{\pi_t}, \tag{15}$$

where $\pi_t = P_t/P_{t-1}$ is gross inflation, while the term $\omega_{j-1}N_{j-1}^{rel}$ is the mass of cohort $j-1$ that died at the end of period $t-1$.

2.2. **Business sector.** The business sector consists of three types of agents: final-good producers, intermediate-goods producers, and investment funds.

2.2.1. *Final good producers.* At every point in time t, a perfectly competitive sector produces a final good y_t by combining a continuum of intermediate goods $y_{i,t}$, $i \in [0, N_t]$, according to the technology $y_t = \left(\frac{1}{N_t}\int_0^{N_t} y_{i,t}^{1/\varepsilon_p}\,\mathrm{d}i\right)^{\varepsilon_p}$, where $\varepsilon_p > 1$ is the (gross) markup parameter. Equivalently, the elasticity of substitution across varieties is $\varepsilon_p/(\varepsilon_p - 1)$, so a higher ε_p corresponds to less substitutable varieties and a larger desired markup. As the population grows, the measure of available intermediate goods expands accordingly, reflecting an increasing mass of variety in production.[5] Final good producing firms take their output price, P_t, and their input prices, $P_{i,t}$, as given and beyond their control. Profit maximization implies $y_{i,t} = (P_{i,t}/P_t)^{-\frac{\varepsilon_p}{\varepsilon_p-1}} y_t$ from which we obtain the relationship between the price of the final good and the prices of intermediate goods $P_t \equiv \left(\frac{1}{N_t}\int_0^{N_t} {P_{i,t}}^{\frac{1}{1-\varepsilon_p}}\,\mathrm{d}i\right)^{1-\varepsilon_p}$.

2.2.2. *Intermediate-goods firms.* Intermediate good i is produced by a monopolistically competitive firm with the following technology:

$$y_{i,t} = (1 - \mathcal{D}(T_t))\,(k_{i,t}^s)^{\alpha}\left(Z_t h_{i,t}\right)^{1-\alpha}, \tag{16}$$

where $\mathcal{D}(T_t)$ is a damage function capturing the impact of climate change on production (specified below), $k_{i,t}^s$ denotes the flow of capital services and $h_{i,t}$ the labour input. The parameter $\alpha \in (0,1)$ measures the output elasticity with respect to capital and Z_t denotes labor productivity. It follows the process $Z_t = (1 + g_{z,t})Z_{t-1}$, where $g_{z,t} = g_{z,t-1}(1-\delta_z)$ is the productivity growth rate and $\delta_z \geq 0$ is the rate of decline in productivity.

During production, firm i generates CO_2 emissions $e_{i,t}$ according to:

$$e_{i,t} = \sigma_t\,(1 - \mu_{i,t})\,y_{i,t}, \tag{17}$$

where $\mu_{i,t} \in [0,1]$ is the abatement effort (i.e., the fraction of emissions abated), $\sigma_t > 0$ represents the emissions per unit of output in absence of any reduction effort and is assumed to decay over time at rate $\delta_\sigma \geq 0$, thus $\sigma_t = \sigma_{t-1}(1-\delta_\sigma)$. Firms may substitute carbon-intensive

[5]The $1/N_t$ normalization inside the aggregator removes love-of-variety effects: a proportional expansion of varieties driven by population growth scales the economy up but does not by itself raise per-capita output. The mass of varieties available in production therefore grows in step with the population without generating endogenous productivity gains.

technologies with low-carbon technologies, but this change in the existing lines of production is costly. We assume that the cost of abatement technology (expressed in units of the final good) is given by:

$$\mathcal{C}^{\mu}_{i,t} = \phi_{1,t}\mu^{\phi_2}_{i,t} y_{i,t}, \tag{18}$$

where $\phi_{1,t} > 0$, and $\phi_2 > 1$ are technological parameters that determine the cost of reducing emissions. In line with the polluter-pays principle, firms face an environmental policy requiring them to pay a carbon price on each unit of emissions, treated as exogenous. Abatement costs are assumed to decline over time at rate $\delta_\phi \geq 0$ due to exogenous technological progress, so that $\phi_{1,t} = \phi_{1,t-1}(1 - \delta_\phi)$.

Intermediate firms set prices subject to Rotemberg adjustment costs:

$$\mathcal{C}^{p}_{i,t} = \frac{\kappa_p}{2}\left(\frac{P_{i,t}}{P_{i,t-1}} - \pi\right)^2 y_t, \tag{19}$$

where $\kappa_p > 0$ is the price stickiness parameter and π is steady-state gross inflation. In period t, nominal profits of a representative firm i are given by

$$P_t d_{i,t} = P_{i,t} y_{i,t} - W_t h_{i,t} - R^k_t k^s_{i,t} - \tau_{e,t} e_{i,t} - P_t \mathcal{C}^{\mu}_{i,t} - P_t \mathcal{C}^{p}_{i,t}, \tag{20}$$

where $\tau_{e,t}$ denotes the exogenous carbon tax while R^k_t is the nominal rental rate of capital services. Thus, the problem faced by firms is that of choosing factor inputs, abatement effort, and their own price so as to maximize the present discounted value of current and expected profits

$$\mathbb{E}_t \left\{ \sum_{s=0}^{\infty} \left(\prod_{\varepsilon=1}^{s} R^{-1}_{t+\varepsilon} \right) P_{t+s} d_{i,t+s} \right\}, \tag{21}$$

subject to demand from final firms and the production function. Intermediate goods firms are assumed to be risk neutral and thus discount future profits at the nominal risk-free rate R_t.

2.2.3. *Investment funds.* Perfectly competitive investment funds use households' savings to buy and manage a portfolio of assets, transferring every period the earned gross return back to households. The portfolio consists of physical capital k_t, bonds b_t (both expressed in per capita terms), and claims on intermediate-good producing firms' profits $d_t = (1/N_t)\int_0^{N_t} d_{i,t}\,\mathrm{d}i$. Investment funds rent capital services to intermediate-good producers. Capital services are defined as

$$k^s_t = u_t k_t, \tag{22}$$

where u_t denotes the capital utilization rate. Adjusting the capital utilization rate is costly and the cost is borne by capital producers. Following Smets and Wouters (2003, 2007), utilization entails the following convex cost (expressed in units of the final good):

$$\mathcal{C}_t^u = \frac{1-\psi_k}{\psi_k} r_k \left[\exp\left(\frac{\psi_k}{1-\psi_k}(u_t - 1) \right) - 1 \right] k_t, \tag{23}$$

where $\psi_k \in (0,1)$ governs the curvature of the cost around the steady state and r_k is the steady-state real rental rate of capital.

A representative investment fund operates to maximize the anticipated present value of future gross returns:

$$\begin{aligned} \mathbb{E}_t \left\{ \sum_{s=0}^{\infty} \left(\prod_{\varepsilon=1}^{s} R_{t+\varepsilon}^{-1} \right) \left[\left(R_{t+s}^k u_{t+s} + (1-\delta) Q_{t+s} \right) k_{t+s} - P_{t+s} \mathcal{C}_{t+s}^u \right. \right. \\ \left. \left. + R_{t-1+s} P_{t-1+s} b_{t+s} + P_{t+s} d_{t+s} \right] \right\} \end{aligned} \tag{24}$$

where δ is the capital depreciation rate, and Q_t is the nominal price of a unit of capital. Risk neutrality justifies discounting at the risk-free rate R_t. As in Bielecki et al. (2023), investment outlays do not appear in the objective: they are financed out of new household savings through the balance-sheet identity below, and only the flows rebated to households enter the maximization.

The nominal balance sheet of investment funds at the end of period t is

$$(1+n) P_t a_{t+1} = Q_t (1-\delta) k_t + P_t i_t + (1+n) P_t b_{t+1}, \tag{25}$$

where i_t denotes investment in physical capital. Physical capital in per capita terms is assumed to accumulate as follows:

$$(1+n) k_{t+1} = (1-\delta) k_t + \left[1 - \kappa_i \left(\frac{i_t}{(1+g_{z,t}) i_{t-1}} - 1 \right)^2 \right] i_t, \tag{26}$$

where $\kappa_i > 0$.

Since investment funds are risk-neutral, their portfolio choices imply equalization of ex-ante rates of return on capital and bonds:

$$\mathbb{E}_t \left\{ \frac{u_{t+1} R_{t+1}^k + (1-\delta) Q_{t+1}}{Q_t} \right\} = R_t. \tag{27}$$

Because all revenues are passed through to households, the ex-post nominal gross return on financial wealth R_t^a is implicitly defined by

$$R_t^a P_{t-1} a_t = \left[u_t R_t^k + (1-\delta) Q_t \right] k_t - P_t \mathcal{C}_t^u + R_{t-1} P_{t-1} b_t + P_t d_t. \tag{28}$$

Equation (28) closes the household-fund block: it pins down R_t^a as the residual gross return that exhausts the investment fund's revenues, and is the rate at which households' financial wealth a_t accumulates in the budget constraint (2).

2.3. **Public sector.** The government collects tax revenue from labor income, financial income, and emissions; spends on public consumption; pays transfers to households; and finances any residual through debt. Its flow budget constraint is

$$\begin{aligned}(1+n) P_t \, b_{t+1}^g = {} & R_{t-1} P_{t-1} \, b_t^g + P_t \, g_t + P_t \, \tau_t \\ & - \tau_h \, W_t h_t - \tau_{a,t} \, (R_t^a - 1) P_{t-1} \, a_t - \tau_{e,t} \, e_t,\end{aligned} \tag{29}$$

where b_t^g is the stock of public debt in per capita terms carried from the previous period, g_t denotes public consumption and is assumed to evolve linearly with aggregate output, while e_t is the aggregate emissions per capita:

$$e_t = \frac{1}{N_t} \int_0^{N_t} e_{i,t} \, \mathrm{d}i. \tag{30}$$

In what follows, carbon tax revenues, $\tau_{e,t} \, e_t$, are either rebated to households as lump-sum transfers or used to reduce labor and/or financial income taxes.

The monetary authority follows a Taylor-type rule by gradually adjusting the nominal interest rate in response to inflation and output growth:

$$\frac{R_t}{R} = \left(\frac{R_{t-1}}{R} \right)^{\varphi_r} \left[\left(\frac{\pi_t}{\pi} \right)^{\varphi_\pi} \left(\frac{y_t}{(1+g_{z,t}) y_{t-1}} \right)^{\varphi_y} \right]^{1-\varphi_r}, \tag{31}$$

where $\varphi_r \in [0,1)$ governs interest-rate smoothing and $\varphi_\pi, \varphi_y > 0$ govern the responses to inflation and output growth.

2.4. **Market clearing conditions, emissions and climate block.** The equilibrium in the final goods market is given by

$$y_t = c_t + i_t + g_t + \mathcal{C}_t^p + \mathcal{C}_t^\mu + \mathcal{C}_t^x + \mathcal{C}_t^u, \tag{32}$$

where all variables are expressed in per capita terms.

The market-clearing conditions for capital and labor are

$$k_t = \frac{1}{N_t} \int_0^{N_t} k_{i,t} \mathrm{d}i \quad \text{and} \quad h_t = \frac{1}{N_t} \int_0^{N_t} h_{i,t} \mathrm{d}i, \tag{33}$$

and the aggregate net supply of bonds is equal to the level of government debt:

$$b_t = b_t^g, \tag{34}$$

where low-case letters refer to per capita values.

Since at the optimum each firm undertakes the same abatement effort, domestic per-capita emissions are determined endogenously as

$$e_t = \sigma_t \left(1 - \mu_t\right) y_t, \tag{35}$$

where $E_t = N_t e_t$ denotes aggregate domestic emissions and μ_t is itself determined endogenously by firms optimizing against the carbon price.

We now turn to the climate block. Following Barrage and Nordhaus (2024), we assume a quadratic damage function that depends on the (global) temperature anomaly:

$$\mathcal{D}(T_t) = \gamma_1 \, T_t + \gamma_2 \, T_t^2. \tag{36}$$

where γ_1 and γ_2 are the coefficients of the process.

To capture the transient climate response, we adopt a parsimonious linear mapping from global emissions to the temperature anomaly, consistent with the evidence reviewed by Dietz et al. (2021). Two variables are taken as exogenous from the DICE-2023 scenarios of Barrage and Nordhaus (2024): the path of total global emissions E_t^{tot} and the carbon tax $\tau_{e,t}$. Conditional on $\tau_{e,t}$, each firm optimally chooses its abatement effort μ_t, so that domestic emissions E_t are determined endogenously in general equilibrium. Rest-of-the-world emissions E_t^* are then simply deduced as the residual:

$$E_t^* = E_t^{tot} - E_t. \tag{37}$$

Temperature evolves according to

$$T_t = T_{t-1} + \xi_T \, E_t^{tot}, \tag{38}$$

where $\xi_T > 0$ governs the transient climate response. All the equilibrium conditions of the model are reported in Appendix A.

3. Calibration

We calibrate the model to the euro area at an annual frequency, taking 2023 as the reference initial date ($t_0 = 2023$).[6] The calibration is disciplined to be consistent with both macroeconomic aggregates and household-level evidence. On the macro side, we target standard euro-area moments. On the micro side, we exploit age-specific moments from the HFCS to pin down life-cycle profiles of income and wealth, which are key to match cohort heterogeneity and age-dependent marginal propensities to consume.

3.1. **Structural parameters.** The structural parameters are calibrated using benchmark values from the literature and empirical estimates drawn from international databases. Table 1 summarizes the calibration. Panel A reports the climate block, largely based on Barrage and Nordhaus (2024), and includes parameters governing the temperature–emissions mapping, the damage function, abatement technology (level and curvature), and the trend in emissions intensity. The damage function $\mathcal{D}(T_t) = \gamma_1 T_t + \gamma_2 T_t^2$ follows the Nordhaus–Barrage specification: the linear coefficient is set to $\gamma_1 = 0$ and the quadratic coefficient to $\gamma_2 = 0.003467$, so that only the quadratic term is active at the calibrated values.

Panel B reports private-sector parameters. We set the annual discount factor to $\beta = 0.99$. The curvature parameter for household portfolio adjustment costs, κ_x, is calibrated to match marginal propensities to consume consistent with the evidence in Christelis et al. (2019). The inverse Frisch elasticity is set to $\nu = 2.21$, following Mouabbi and Sahuc (2019). On the production side, the capital share α is set to 0.3 to match the average capital share in net (of fixed costs) output (McAdam and Willman, 2013). The depreciation rate of capital, δ, is set to 0.05, as detailed by European Central Bank (2006). The gross markup of 1.33 is based on estimates from Christopoulou and Vermeulen (2012) and Kouvavas et al. (2021). The investment adjustment cost parameter, κ_i, is set to 5.28 following Mouabbi and Sahuc (2019). Nominal rigidities (price-adjustment costs) are calibrated to be in line with estimates from Druant et al. (2012) and Gautier et al. (2024). Following Keen and Wang (2007), a quarterly price adjustment frequency of 25 percent corresponds to an annualized Rotemberg adjustment cost parameter of 2.024. Finally, steady-state gross inflation is calibrated to $\pi = 1.02$, in line with the ECB's medium-term inflation target of 2 percent.

Panel C details the parameters governing fiscal policy and monetary feedback rules. The steady-state ratios of government spending and public debt to GDP are calculated from data in the ECB Statistical Data Warehouse (European Central Bank, 2024) over the 1999–2023

[6] This corresponds to the EA20 (20 member states after Croatia's accession on 1 January 2023).

TABLE 1. Model parameters

Name	Symbol	Value	Sources
Panel A: Climate parameters			
Atmospheric conversion	ξ_T	5.4545×10^{-4}	Own calculations
Linear damage coefficient	γ_1	0	Barrage and Nordhaus (2024)
Quadratic damage coefficient	γ_2	0.003467	Barrage and Nordhaus (2024)
Abatement cost curvature	ϕ_2	2.600	Barrage and Nordhaus (2024)
Decay rate of abatement cost	δ_ϕ	0.017	Barrage and Nordhaus (2024)
Decay rate of emission intensity	δ_σ	0.000	Barrage and Nordhaus (2024)
Panel B: Structural parameters			
Population growth rate (%)	n	0.220	United Nations (2024)
Discount factor	β	0.990	Standard
Inverse of the Frisch elasticity of labor supply	ν	2.210	Mouabbi and Sahuc (2019)
Portfolio adjustment cost curvature	κ_x	0.040	Own calculation
Decay rate of productivity	δ_z	0.017	Barrage and Nordhaus (2024)
Capital depreciation rate	δ	0.050	European Central Bank (2006)
Capital share in output	α	0.300	McAdam and Willman (2013)
Investment adjustment cost curvature	κ_i	5.280	Mouabbi and Sahuc (2019)
Gross markup	ϵ_p	1.333	Christopoulou and Vermeulen (2012)
Price stickiness	κ_p	2.024	Gautier et al. (2024)
Panel C: Public sector parameters			
Share of government purchases in GDP	g/y	0.210	European Central Bank (2024)
Steady-state government bonds to GDP ratio	b/y	0.540	European Central Bank (2024)
Labor income tax	τ_h	0.178	OECD (2025)
Financial income tax	τ_a	0.337	Bachas et al. (2024)
Interest rate smoothing	φ_r	0.833	Own calculations
Reaction to inflation	φ_π	1.925	Own calculations
Reaction to GDP growth	φ_y	0.706	Own calculations
Gross inflation rate	π	1.020	European Central Bank's target

sample. The labor tax rate, defined as the income tax as a percentage of gross wage earnings, is obtained as a GDP-weighted average of the euro-area member states reported in OECD (2025). The financial income tax rate is computed as the weighted average of the effective tax rate on capital reported by Bachas et al. (2024) for the same countries used in the labor tax calculation. The parametrization of the monetary policy rule is based on the estimation of a log-linearized version of Equation (31), using euro-area data for the period 1990-2023 from an updated version of the Area Wide Model database (Fagan et al., 2005), converted to annual frequency.

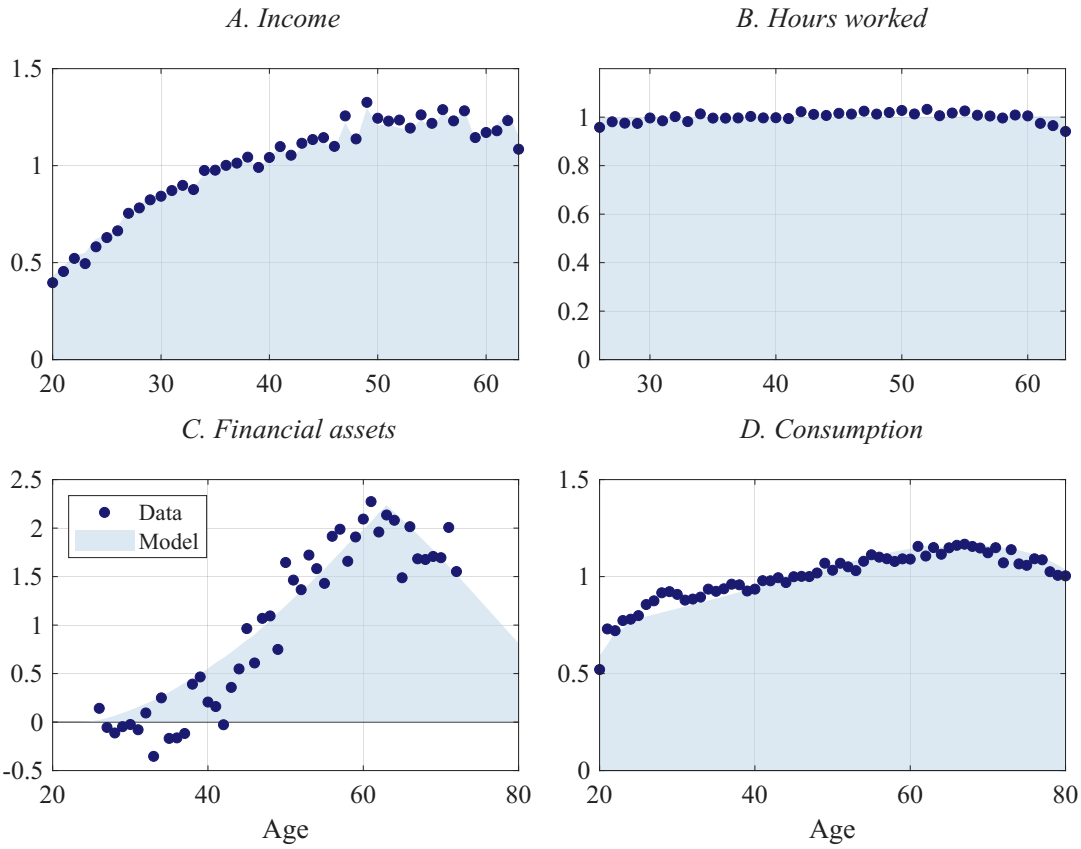
3.2. **Life-cycle profiles.** We use individual data from the Household Finance and Consumption Survey hosted by the European Central Bank (`https://www.ecb.europa.eu/stats/ecb_surveys/hfcs/html/index.en.html`). The survey collects detailed information on household finances, including real assets and their financing, other liabilities and credit constraints, private businesses, financial assets, income, and consumption (see HFCN, 2023, Annicchiarico et al., 2025). The HFCS has been conducted in four waves (2010, 2014, 2017, and

2021) among households in all euro-area member countries. In the most recent wave, more than 83,000 households were interviewed. We average the results across the four waves to obtain estimates representative of roughly a decade. All monetary amounts are expressed in constant 2021 euros, deflated using the harmonised index of consumer prices (see Appendix B). We focus on three variables (HFCS code in parentheses): *(i)* labor income, defined as the sum of employee income (DI1100) and self-employment income (DI1200); *(ii)* hours worked, defined as weekly hours worked in the main job (PE0600), set to zero for non-workers; and *(iii)* financial assets, defined as the sum of deposits (DA2101), mutual funds (DA2102), bonds (DA2103), the value of non-self-employment private business (DA2104), publicly traded shares (DA2105), life insurance (DA2109), and business wealth (DA1200), minus the outstanding balances of mortgage (DL1100) and non-mortgage (DL1200) debt. These definitions are chosen to map the HFCS variables as closely as possible into the objects in the model. In particular, our measure of financial assets is a model-consistent net financial wealth concept and therefore differs from the broader measure of total assets reported in the introduction. While calibrating the model, we match the steady-state age profiles of labor income and hours worked exactly to their empirical counterparts by setting the age-specific productivity parameters z_j equal to the empirical ratio of labor income to hours worked.

Figure 2 presents the empirical and model-implied profiles. The income profile (Panel A) displays the canonical hump shape, peaking around ages 50-55 before declining toward retirement, and the model tracks it closely. Hours worked (Panel B) are remarkably flat over the working life, suggesting a weak intensive-margin response to the income profile and leaving most of the life cycle adjustment to savings rather than labor supply. Financial assets (Panel C) follow the textbook Modigliani pattern: negative net positions in the twenties reflecting borrowing, a steep accumulation phase through midlife, and a peak around age 60-65. The model reproduces the broad shape of the accumulation profile quite well despite abstracting from borrowing entirely, a restriction that mechanically rules out the negative asset positions observed among young households in the data yet leaves the overall fit largely intact. Consumption (Panel D) rises monotonically through most of the life cycle before declining slightly in old age, departing from the flat profile implied by the permanent income hypothesis and pointing to liquidity constraints early in life or precautionary saving motives, a pattern the model replicates without directly targeting it.

3.3. **Demography.** We use data from the 2024 revision of the United Nations' World Population Prospects (`https://population.un.org/wpp/`) to calibrate population growth and

FIGURE 2. Life cycle profiles in the euro area



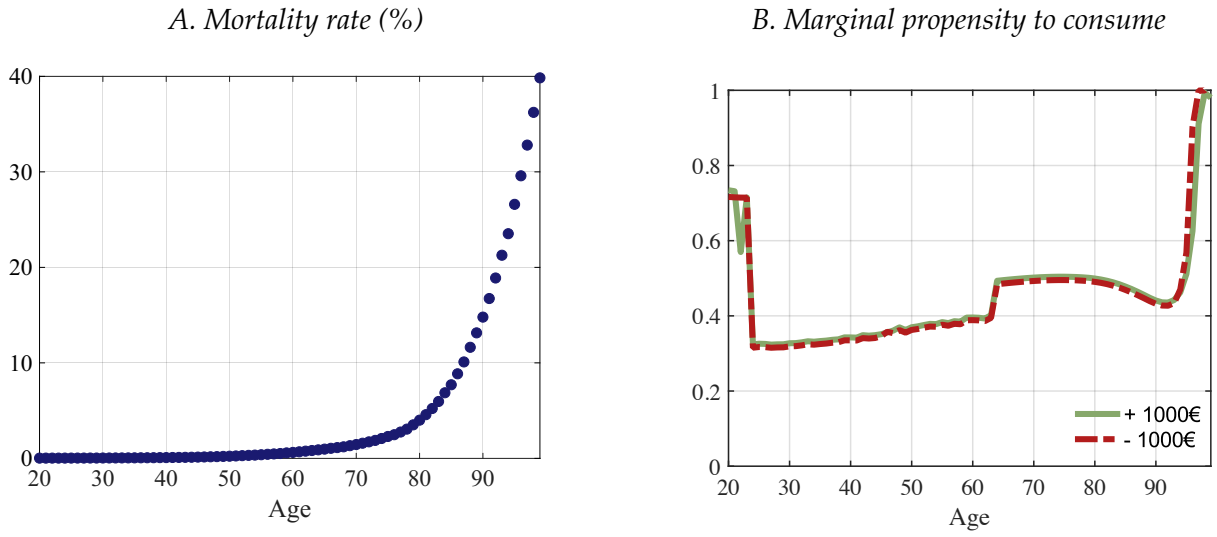
Notes: The panels show age profiles from the HFCS raw data (dots) and model-implied smoothed profiles (areas). All series are normalized by their average values over the working age (income and hours worked) or lifecycle (financial assets and consumption). Raw data were adjusted for household size and aggregated by cohort.

age-dependent mortality risk. The population growth rate is set to $n = 0.22\%$, matching the average growth rate of the total euro area population observed over the period 2010-2023. We assume a constant population structure, implying that the cohort aged 20 and the total population grow at the same rate. Age-specific mortality rates are constructed using the 2023 country-level Life Tables and corresponding cohort population data (Figure 3, Panel A).

3.4. **Marginal propensity to consume over the life cycle.** The model generates a pronounced life-cycle pattern of marginal propensities to consume (MPCs) that is central to the distributional effects of the transition. We simulate an unexpected, transitory €1,000 income shock in 2025 and compute the share consumed on impact by each age cohort (Figure 3, Panel B).[7]

[7]For the purpose of this experiment, the household budget constraint (2) is augmented with a cohort-specific transitory income shock $\epsilon_{j,t}$, so that the cash flow becomes $x_{j,t} = (1-\tau_h)\,\mathcal{I}_{j<JR}\,(W_t/P_t)\,z_j h_{j,t} + beq_t + \tau_{j,t} + \epsilon_{j,t} - c_{j,t}$. The shock $\epsilon_{j,t}$ is a one-time €1,000 transfer to cohort j in 2025; it is zero in all other periods, in the steady state, and along all policy-experiment paths considered elsewhere in the paper. The cohort-level MPC reported in Figure 3, Panel B, is the impact response of $c_{j,t}$ to $\epsilon_{j,t}$.

FIGURE 3. Mortality rate and marginal propensity to consume over the life cycle



Notes: Panel A plots the mortality rates in 2023 (United Nations, 2024). Panel B displays the marginal propensity to consume (MPC) out of a transitory idiosyncratic income shock of €1,000 by age cohort, computed from the calibrated model following an unexpected shock in 2025. The MPC is defined as the ratio of the contemporaneous consumption response to the income shock.

MPCs are high at both ends of the life cycle for distinct reasons, implying imperfect aggregate insurance. Young households exhibit high MPCs because they hold little wealth and face a binding borrowing constraint. As a result, they behave hand-to-mouth: income shocks translate almost one-for-one into consumption. Negative shocks, such as wage compression from carbon pricing, are therefore expected to reduce consumption immediately and permanently. At older ages, MPCs rise due to end-of-life decumulation. As survival probabilities decline, the incentive to save weakens, and households consume a larger share of additional income. At intermediate ages, the model features wealthy hand-to-mouth households in the spirit of Kaplan and Violante (2014). These households hold illiquid assets but face short-run liquidity constraints due to portfolio adjustment costs, leading them to exhibit high MPCs despite positive wealth. This group is consistent with euro-area evidence from the HFCS and reinforces incomplete insurance, as even wealthy households respond strongly to income shocks. This MPC profile has two implications for the green-transition analysis that follows. First, aggregation is non-trivial: a representative-agent setup would average across cohorts and miss the heterogeneity. Second, any policy that redistributes income across age groups produces heterogeneous consumption responses, since cohorts with different MPCs absorb income changes to different extents.

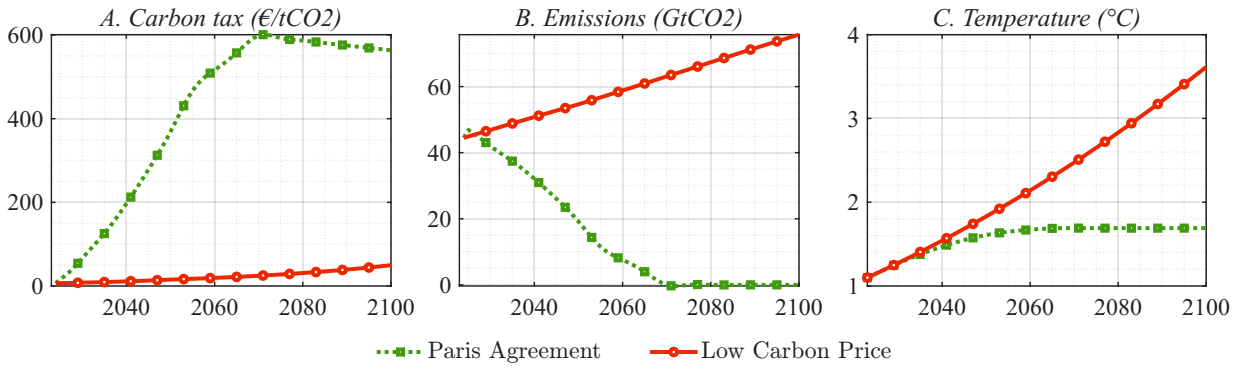
4. The aggregate effects of the green transition

This section characterizes the aggregate dynamics of the green transition under alternative carbon pricing paths. Comparing these scenarios reveals how climate policy transmits to aggregate variables over the transition and highlights the two opposing forces, *i.e.*, wage compression and the rise in financial wealth returns, that together define the redistribution force analyzed in Section 5.

4.1. **Solution method and exogenous global climate paths.** To solve the model, we rely on a perfect foresight solution method. The algorithm computes paths for endogenous variables consistent with the model's equations by solving the resulting simultaneous equation system via a Newton-type method, given a sequence of exogenous transition paths and the absence of aggregate uncertainty. This approach captures all nonlinearities of the model while remaining computationally tractable over the long horizons required by the transition analysis.

Our analysis relies on long-term projections generated by the model to explore alternative trajectories for the euro area up to 2100. Specifically, we assume that in 2023, agents receive information about a long-term carbon tax path. The *Paris Agreement* scenario implements a carbon tax consistent with limiting global warming to below 2°C above pre-industrial levels. The *Low Carbon Price* scenario extrapolates current policies as of 2023, with a global average carbon price of \$6/tCO_2 growing at 2.5% annually. These correspond to the "R=1%" and "Base" cases in Barrage and Nordhaus (2024), respectively.

Figure 4. Exogenous global climate paths



Notes: The figure reports the exogenous carbon tax paths (in euros per ton of carbon) and the resulting world emissions and temperature trajectories under the *Paris Agreement* ("R=1%") and *Low Carbon Price* ("Base") scenarios, taken from the DICE-2023 framework of Barrage and Nordhaus (2024).

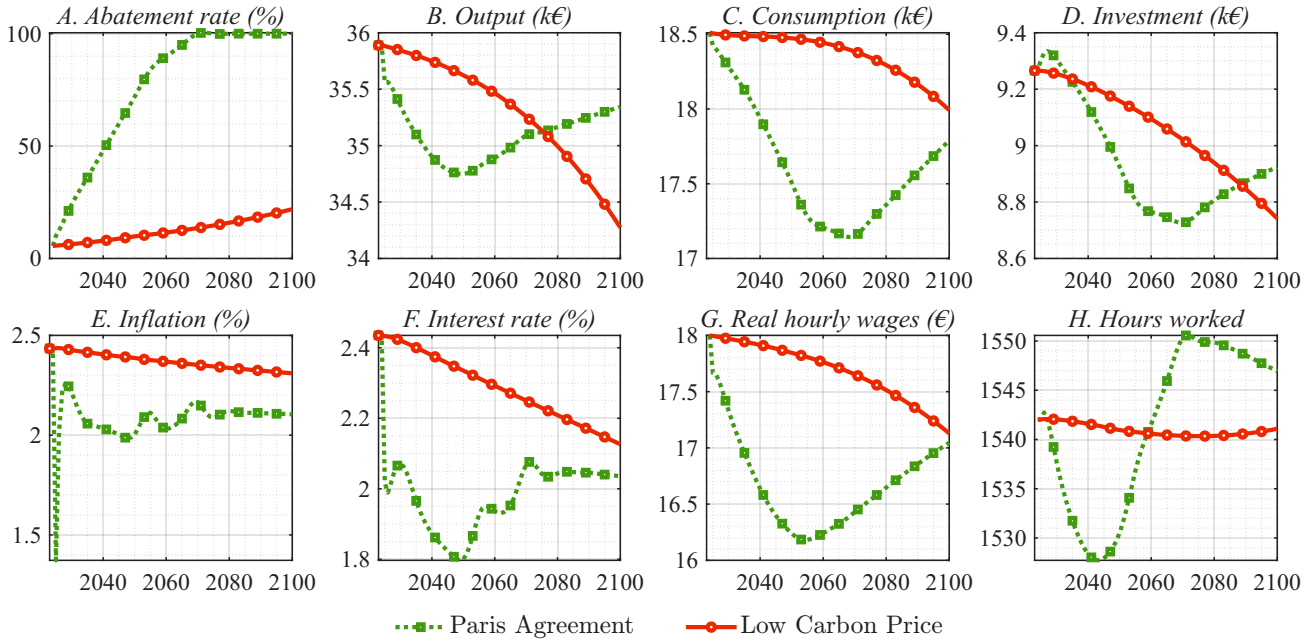
We treat as exogenous both the carbon tax path (in euros per ton of CO_2) and the trajectory of global emissions, from which temperature is directly derived from Equation (38). Conditional on these inputs, euro-area abatement is determined endogenously by firms optimizing against the carbon tax. The model then solves jointly for euro-area emissions, output, factor prices, inflation, and asset returns, which together determine the distributional incidence of the transition across cohorts. This strategy leaves the optimal determination of the carbon tax schedule and transition path outside the scope of the model, instead treating the tax trajectory as given by global climate commitments. Our focus is therefore on tracing how a predetermined carbon tax path transmits through the euro-area economy and generates distinct welfare dynamics across cohorts, rather than on solving for an optimal climate policy. Figure 4 reports the exogenous carbon tax paths under the two scenarios, together with the resulting global emissions and temperature trajectories.

4.2. **Model-implied projections under CO_2 emissions scenarios.** We characterize the macroeconomic transition implied by alternative carbon pricing paths by comparing the Paris Agreement scenario to a *Low Carbon Price* alternative. In both scenarios, carbon tax revenues are returned equally to households via lump-sum transfers. Figure 5 shows the simulation results for eight main macroeconomic variables over 2023-2100.[8] The two scenarios primarily differ in the intensity of abatement. Under the Paris-consistent path, firms progressively scale up abatement efforts until emissions are nearly eliminated by the end of the century. In contrast, under low carbon pricing, abatement remains negligible throughout.

Consistent with Sahuc et al. (2024) and Jondeau et al. (2026), the stronger carbon tax induces a contraction in economic activity by 3.5% in the short run. Output declines as higher production costs compress firm margins and reduce labor demand. This contraction is not driven by intertemporal substitution: real interest rates fall during the transition, which would by itself push consumption up. Instead, it reflects a direct income effect. Lower labor income and profits reduce households' disposable income, leading to a decline in consumption. Both consumption and investment fall (-7% and -5%, respectively). The carbon tax originates as a supply-side shock, but the simultaneous decline of both demand components indicates that the adjustment operates primarily through aggregate demand. Firms reduce investment in response to weaker demand and lower profitability, but the fall in consumption is more pronounced. This is a distinctive feature of the model that reflects its OLG structure, as discussed below.

[8] All real variables are expressed in detrended per capita units, normalizing out population and productivity trend growth to isolate the purely transitional effects of climate policy.

FIGURE 5. Transition dynamics under alternative climate policy paths



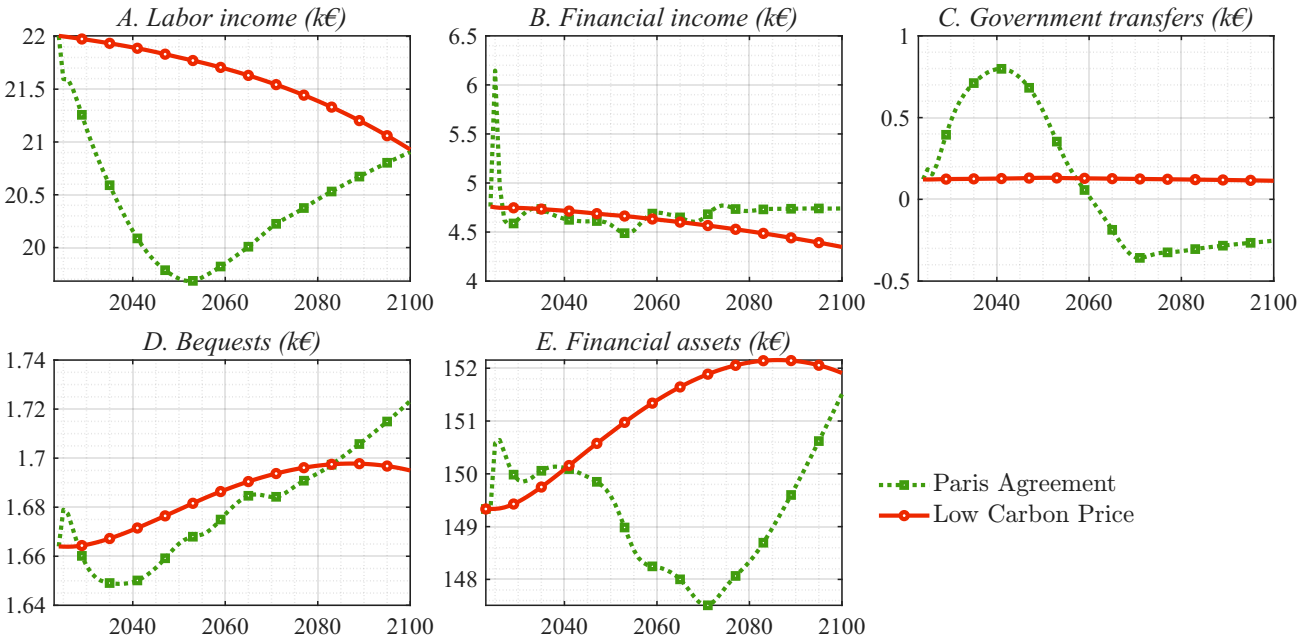
Notes: The figure reports transition paths under the *Paris Agreement* ("R=1%", dashed green line) and *Low Carbon Price* ("Base", red plain line) scenarios, taken from the DICE-2023 framework of Barrage and Nordhaus (2024). All variables are expressed in detrended levels.

Relative to the *Low Carbon Price* scenario, the Paris Agreement generates substantially stronger disinflationary pressure. In particular, the announcement of the steeper carbon tax path triggers a sharp initial decline in inflation at the onset of the transition. This abrupt disinflation reflects the forward-looking contraction in aggregate demand: because households and firms immediately internalize the future increase in carbon prices, consumption and investment fall on impact, reducing firms' marginal costs and inflationary pressures. Inflation subsequently remains below the *Low Carbon Price* path, gradually converging from around 2.4 percent in 2023 to 2 percent by mid-century before partially recovering. Nominal interest rates decline in tandem, consistent with the monetary policy rule.

In the long run, under the *Paris Agreement*, the economy gradually recovers as the capital stock adjusts and climate damages are contained. Under the *Low Carbon Price* scenario, the absence of mitigation leads to rising damages, which weigh on productivity and reduce long-run output. The transition can therefore be understood as a temporal trade-off: a front-loaded economic cost in exchange for long-term resilience. The short-run contraction is the price of avoiding a more persistent decline in economic performance in the future.

4.3. **The redistribution force of climate policy.** Climate policy affects household income through two distinct channels, which together define a *redistribution force*. The first operates

FIGURE 6. Household budget decomposition and financial assets



Notes: The figure plots the difference between the *Paris Agreement* and the *Low Carbon Price* scenarios for key components of the household budget: labor income, financial income, government transfers, and bequests. All variables are expressed in efficient per capita units.

through *labor income*. Higher carbon prices increase production costs and depress aggregate demand, reducing labor demand and compressing wages. Because capital is predetermined in the short run, the incidence of abatement costs falls disproportionately on labor. This channel reduces household income and consumption. The second channel operates through *financial wealth*. The announcement of a steeper carbon tax path generates an initial disinflationary shock, reflecting the forward-looking contraction in aggregate demand at the onset of the transition. This unexpected decline in inflation has two effects: *(i)* it raises the real value of nominal financial assets, generating capital gains for asset holders; and *(ii)* it increases the real return on financial wealth.[9] Through this *financial-wealth channel*, household income and consumption rise. These two channels therefore operate in opposite directions. The labor-income channel reduces purchasing power, while the financial-wealth channel increases it. The overall effect on household income depends on their relative strength.

Quantitatively, the labor-income channel dominates. Figure 6 decomposes the household budget into its main components and shows that labor income declines sharply and persistently during the transition in the *Paris Agreement* scenario, particularly in the early decades

[9]This second effect arises because the return on financial wealth depends, among other things, on the price of capital (see Equation 28), which reflects the expected return on physical capital discounted by risk-neutral investment funds. Following the initial disinflation, investment funds discount expected returns at a lower nominal rate, causing the price of capital to jump on impact and increasing the return on financial wealth.

(-10% between 2023 and 2050). The wage compression reflects the carbon tax's dual effect on firms: it erodes profits and dampens labor demand. As discussed in the next section, this wage effect is the main driver of the redistributive consequences of climate policy.

By contrast, gains from the financial-wealth channel are smaller and insufficient to offset aggregate income losses. The sharp initial disinflation generated by the announcement of the carbon tax path raises the real value of nominal assets and the real return on financial wealth. However, these effects fade as inflation expectations adjust over the transition. Finally, government transfers and bequests respond only modestly by comparison. Transfers fluctuate temporarily, reflecting fiscal adjustments, but do not drive the bulk of the income dynamics. Bequests evolve smoothly and mainly reflect the mechanical accumulation of wealth.

This dominance of the labor-income channel reflects structural features of the economy. First, the short-run incidence of the carbon tax falls on labor because capital cannot adjust immediately. Capital adjusts intertemporally through investment, while labor markets clear within the period. The short-run incidence of the carbon tax therefore concentrates on wages, reinforcing the labor-income channel for working cohorts. Second, portfolio adjustment frictions limit households' ability to benefit from changes in asset returns. This illiquidity dampens the financial-wealth channel for middle-aged cohorts who might otherwise capture transitional gains through rapid portfolio reallocation, extending the quantitative dominance of the labor-income channel beyond what factor endowments alone would predict. Third, differences in marginal propensities to consume amplify the impact of income shocks, particularly for households relying on labor income. The no-borrowing constraint (5), combined with the hump-shaped income profile calibrated to the HFCS, generates a U-shaped MPC profile over the life cycle. Young households translate labor income losses nearly one-for-one into reduced consumption, while a population of wealthy hand-to-mouth households at intermediate ages, in the spirit of Kaplan and Violante (2014), ensures that the transition remains imperfectly insurable even for cohorts with non-negligible wealth.

These mechanisms together define a redistribution force inherent to climate policy. Even in the aggregate, carbon pricing shifts income away from labor toward capital. In the presence of life-cycle heterogeneity, this force translates into systematic intergenerational redistribution, which we analyze next.

5. Intergenerational redistribution dynamics

We now examine how the effects of the transition are distributed across cohorts. The overlapping-generations structure of the model allows us to trace how the costs and benefits of climate policy are allocated over the life cycle, depending on households' exposure to labor income and financial assets. Because younger cohorts rely primarily on labor income, while older cohorts hold a disproportionate share of financial wealth, the two channels identified above translate directly into heterogeneous welfare outcomes across age groups.[10] We quantify these intergenerational effects by comparing cohort-specific lifetime welfare under the *Paris Agreement* and *Low Carbon Price* scenarios.

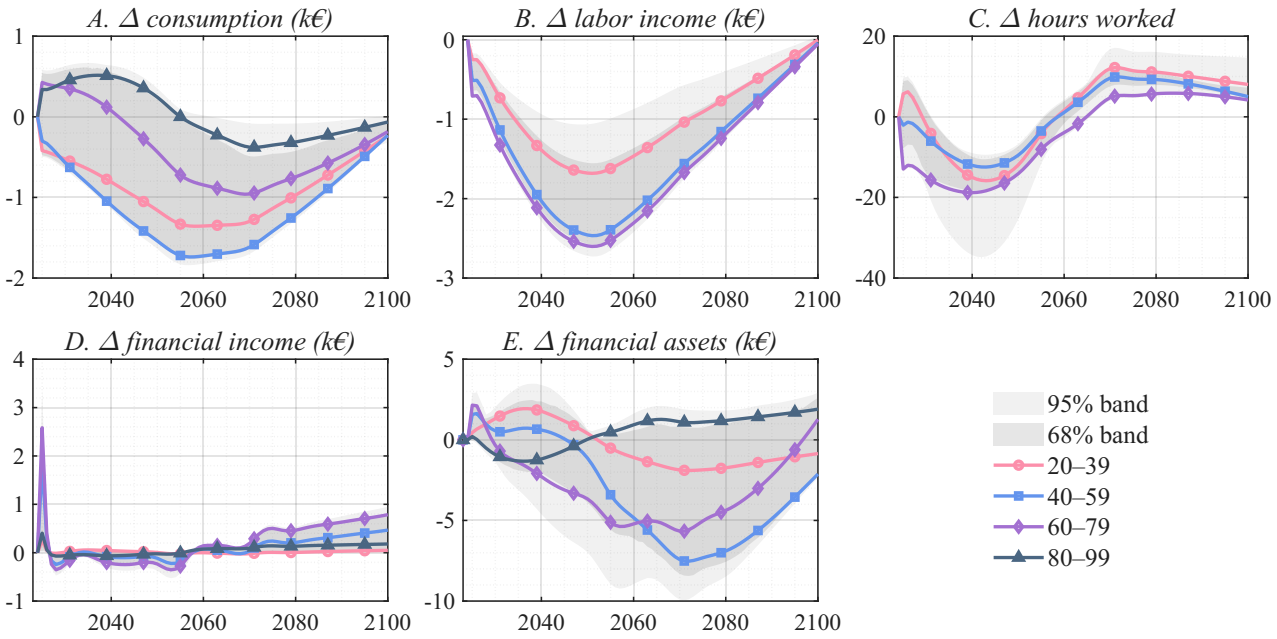
5.1. **Age-dependent effects of the green transition.** We first study how the aggregate dynamics translate into heterogeneous outcomes across cohorts. Figure 7 reports the difference between the *Paris Agreement* and *Low Carbon Price* scenarios by age group (20–39, 40–59, 60–79, 80–99).

A clear age gradient emerges. Younger and middle-aged cohorts experience large and persistent consumption losses over the transition, whereas the oldest cohorts are largely insulated and may even record small gains in the early decades. This heterogeneity reflects differential exposure to the labor-income channel. Labor-income losses are largest for cohorts aged 20–59, who supply the bulk of labor when the carbon tax is introduced, and decline sharply for older cohorts. Importantly, hours worked respond only modestly across cohorts, indicating that the decline in labor income is driven primarily by lower real wages rather than labor-supply adjustments.

The financial-wealth channel provides only a partial offset. All cohorts experience a temporary increase in financial income at the onset of the transition, reflecting the revaluation of nominal wealth following the disinflation surprise, with gains concentrated among the 60–79 and 80–99 cohorts who hold the bulk of financial assets. Quantitatively, however, this effect remains small and short-lived relative to the persistent decline in labor income. Asset dynamics subsequently diverge across age groups. Cohorts aged 20–59 reduce net saving and progressively decumulate financial assets to smooth consumption in response to persistent labor-income losses, leading to a marked deterioration in their balance sheets over the transition. Cohorts aged 80–99 remain largely insulated from labor-income losses and preserve, or even strengthen, their financial positions throughout. Cohorts aged 60–79 occupy

[10] In Appendix C, Figure C.1 reports the age profile of labor income as a share of total income in the pre-transition steady state.

FIGURE 7. Age-dependent distributional effects of the green transition



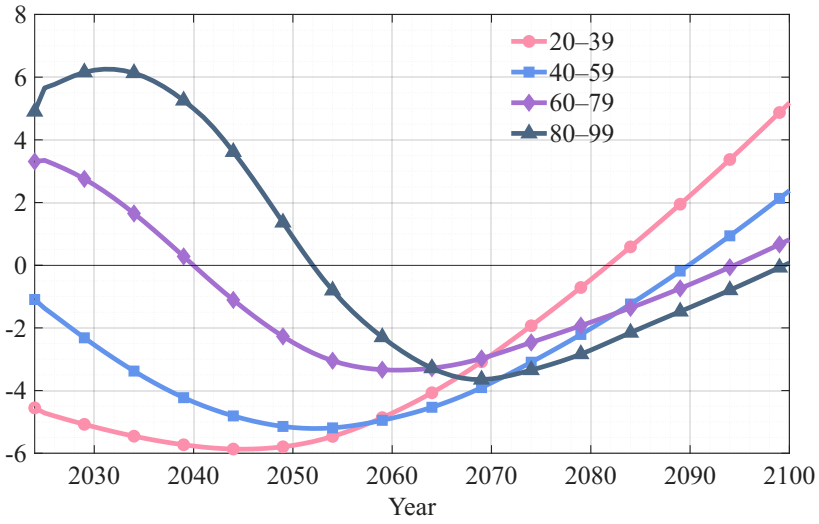
Notes: The figure reports the difference between the *Paris Agreement* and the *Low Carbon Price* scenarios for consumption, labor income, hours worked, financial income, and financial assets. Cohorts are grouped by age (20–39, 40–59, 60–79, 80–99). Shaded areas denote the cross-sectional distribution across households within each cohort: dark bands correspond to the 68% interval and light bands to the 95% interval. All real variables are expressed in efficient per capita units.

an intermediate position: they partially offset labor-income losses through financial wealth gains, but nonetheless progressively liquidate asset holdings to sustain consumption as the transition unfolds.

Figure 7 illustrates that the dominance of the labor-income channel at the aggregate level maps into systematic differences over the life cycle. Cohorts that rely more heavily on labor income bear the bulk of the adjustment costs, while those with greater exposure to financial income are partially insulated. The ability to self-insure (although imperfectly, given the portfolio frictions) through assets therefore shapes the distributional incidence, reinforcing consumption asymmetries between younger and older cohorts. This mechanism is the key driver of intergenerational redistribution.

5.2. **Welfare effects over the transition.** We now turn to welfare effects. The heterogeneous income and asset dynamics documented above translate into cohort-specific welfare effects that depend on both exposure and timing over the life cycle. To quantify these intergenerational effects, we compute, for each cohort, a consumption-equivalent welfare measure (CEV), defined as the proportional change in remaining lifetime consumption that makes households indifferent between the *Paris Agreement* and the *Low Carbon Price* scenarios.

FIGURE 8. Consumption-equivalent variation from the green transition



Notes: The figure reports the consumption-equivalent variation $\Im_{j,t}$ across cohorts (20–39, 40–59, 60–79, 80–99) along the green transition path. $\Im_{j,t}$ is the proportional shift in the *Low Carbon Price* baseline consumption stream required to match lifetime utility under the *Paris Agreement*. The vertical axis measures the magnitude of the consumption-equivalent variation in percent of baseline consumption.

Let $s \in \{\text{PA}, \text{LCP}\}$ denote the policy scenario, and let $\mathcal{W}^s_{j,t}$ denote the lifetime welfare of cohort j at time t under scenario s, as defined in Equation (1). The consumption-equivalent variation $\Im_{j,t}$ solves:

$$\mathcal{W}^{\text{PA}}_{j,t} = \mathbb{E}_t \left\{ \sum_{k=0}^{J-j} \beta^k \frac{N_{j+k,t+k}}{N_{j,t}} \left(\log\left((1+\Im_{j,t}) c^{\text{LCP}}_{j+k,t+k} \right) - \varphi_{j+k} \frac{(h^{\text{LCP}}_{j+k,t+k})^{1+\nu}}{1+\nu} \right) \right\}. \tag{39}$$

A positive value of $\Im_{j,t}$ indicates that cohort j prefers the *Paris Agreement*, while a negative value indicates a welfare loss relative to the *Low Carbon Price* scenario.

Figure 8 reports the resulting welfare profiles by age groups.[11] The welfare effects of the green transition exhibit a rich intergenerational pattern driven by differences in exposure and horizon. The transition initially redistributes welfare toward older cohorts, who benefit from higher financial wealth, while younger and middle-aged cohorts incur losses due to their greater exposure to labor income declines. This initial redistribution reverses over time. As the transition progresses, all cohorts experience welfare losses reflecting the aggregate cost of adjustment. In the long run, however, welfare recovers as the benefits from lower climate

[11] Aggregating individual CEVs across age bands requires care: the discount factor $\sum_{k=0}^{J-j} \beta^k N_{j+k,t+k}/N_{j,t}$ shrinks mechanically with age and inflates the CEV of older cohorts. We address this by weighting each cohort's CEV by both its population share and its remaining lifetime. For a band $\mathcal{G}(t)$ of cohorts alive at time t, the aggregated CEV is $\overline{\Im}_{\mathcal{G},t} = \sum_{j \in \mathcal{G}(t)} \varrho_{j,t} \Im_{j,t}$, with $\varrho_{j,t} = (J-j+1) N^{rel}_j / \sum_{j \in \mathcal{G}(t)} (J-j+1) N^{rel}_j$, where $J-j+1$ is the remaining lifetime of cohort j. This downweights cohorts with few remaining periods.

damages materialize, disproportionately benefiting younger cohorts with longer horizons.[12] Cohorts with longer horizons internalize a larger share of the reduction in future climate damages, while older cohorts are largely insulated from these gains due to their shorter remaining lifetime.

These mechanisms imply that the welfare effects of climate policy cannot be understood without accounting for both the timing of shocks and the life-cycle composition of income and wealth. Their interaction is central to the intergenerational redistribution induced by the transition. The *Paris Agreement* shifts short-run benefits toward older cohorts through the financial-wealth channel, while delaying the climate dividend to younger and future cohorts through the labor-income channel.

6. Carbon tax revenue recycling

The previous section showed that the green transition generates a systematic redistribution across cohorts through the interaction of the labor-income and financial-wealth channels. We now examine how fiscal policy can attenuate or amplify these forces through the recycling of carbon revenues. We consider two recycling schemes: a reduction in labor income taxation, which primarily benefits working-age households, and a reduction in financial income taxation, which benefits asset-rich retired cohorts. We show that the choice of recycling instrument generates a tight trade-off between efficiency, intergenerational compensation, and inequality.

6.1. Double dividends through tax cuts.

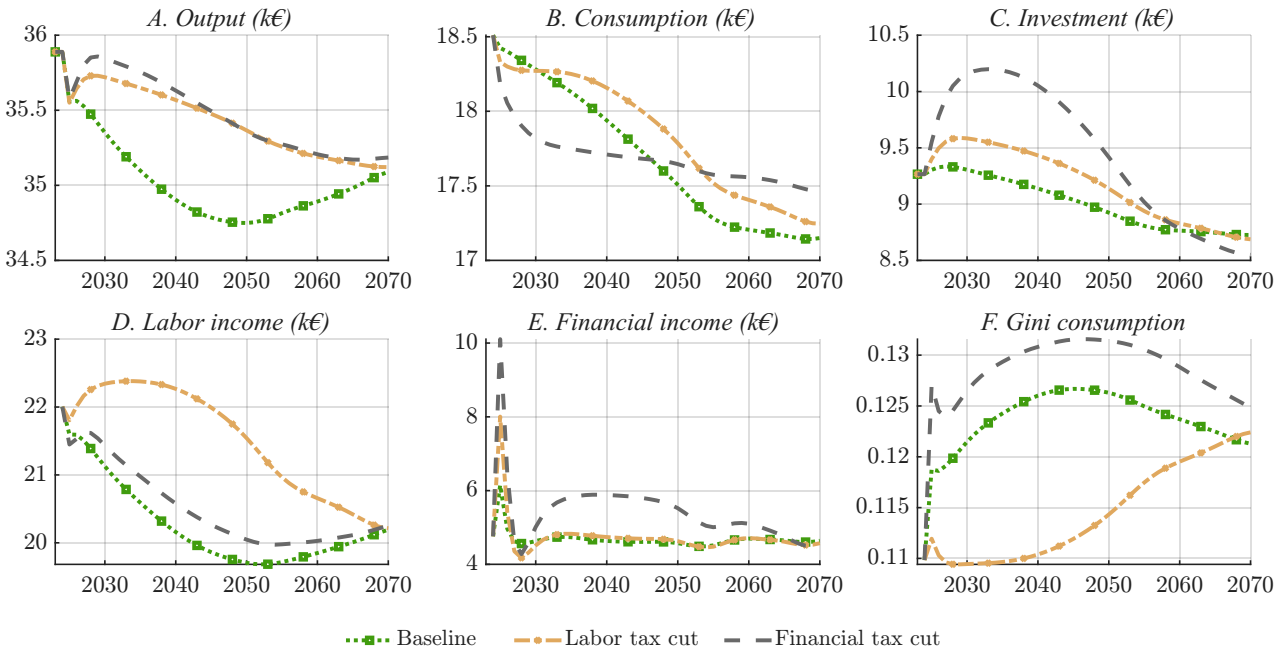
We begin by evaluating the extent to which carbon revenue recycling through tax cuts can generate a double dividend, i.e., simultaneously mitigate the macroeconomic cost of the transition and improve distributional outcomes (Goulder, 1995, Bovenberg and Heijdra, 1998).

To this end, we consider two alternative revenue-neutral recycling schemes that allocate carbon revenues across labor income tax cuts and financial income tax cuts. These instruments operate through different margins of the economy and interact with the two redistribution channels identified in Section 5. In the first scheme, a fraction $\zeta_L \in [0,1]$ of revenues is rebated through a cut in the labor tax rate:

$$(\tau_w - \tau_{w,t}) W_t h_t = \zeta_L \tau_{e,t} e_t, \tag{40}$$

[12] Appendix D complements these findings by showing the full age distribution of the CEVs for different years over the transition.

FIGURE 9. Aggregate effects of alternative carbon revenue recycling schemes



Notes: The figure displays transition paths under the *Paris-Agreement* scenario for three carbon revenue recycling schemes: baseline (lump-sum transfers to households), labor income tax cut, and financial income tax cut. The Gini coefficient in Panel F is computed over the cross-sectional distribution of per capita consumption across all living cohorts at each date, and ranges from 0 (perfect equality) to 1 (maximum inequality).

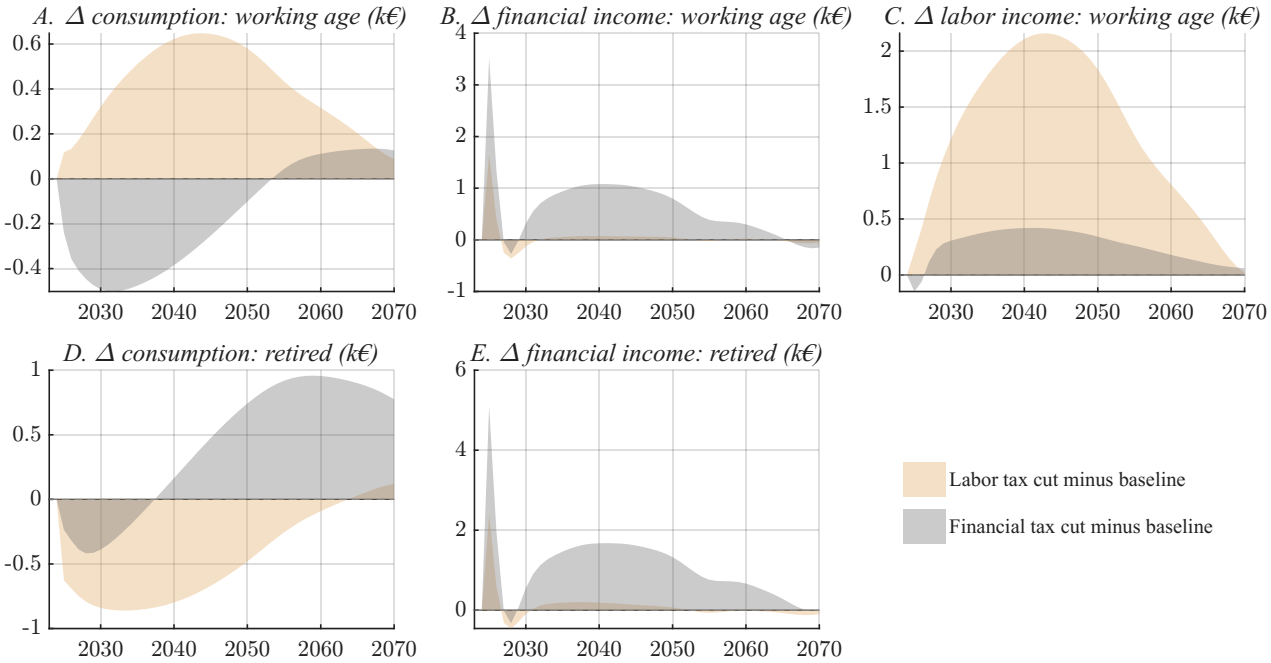
so that $\zeta_L = 0$ corresponds to the baseline lump-sum scheme and $\zeta_L = 1$ implements a full labor double dividend. In the second scheme, a fraction $\zeta_F \in [0,1]$ is instead rebated through a cut in the financial tax rate:

$$(\tau_a - \tau_{a,t})(R_t^a - 1)P_{t-1}a_t = \zeta_F \tau_{e,t} e_t. \tag{41}$$

Figure 9 reports the aggregate dynamics under these alternative schemes. The labor tax cut operates through the labor-income channel. By lowering the tax wedge on wages, it increases after-tax labor income and partially offsets the decline in pre-tax wages, leading to a sustained improvement in labor income for working-age households relative to baseline. The resulting increase in disposable income supports consumption and, by redirecting resources toward households with higher marginal propensities to consume, sustains aggregate demand. Output and consumption both exceed their baseline paths. The distributional cost is borne by retired cohorts. As shown in Figure 10, consumption of retired households falls relative to baseline, translating into persistent welfare losses (Figure 11). The scheme thus improves efficiency, but at the cost of an intergenerational transfer away from retirees.

The financial tax cut operates through the return on assets, and therefore it reinforces the financial-wealth channel. By raising the after-tax return to saving, it increases the value of

FIGURE 10. Redistribution intensity of alternative carbon revenue recycling schemes

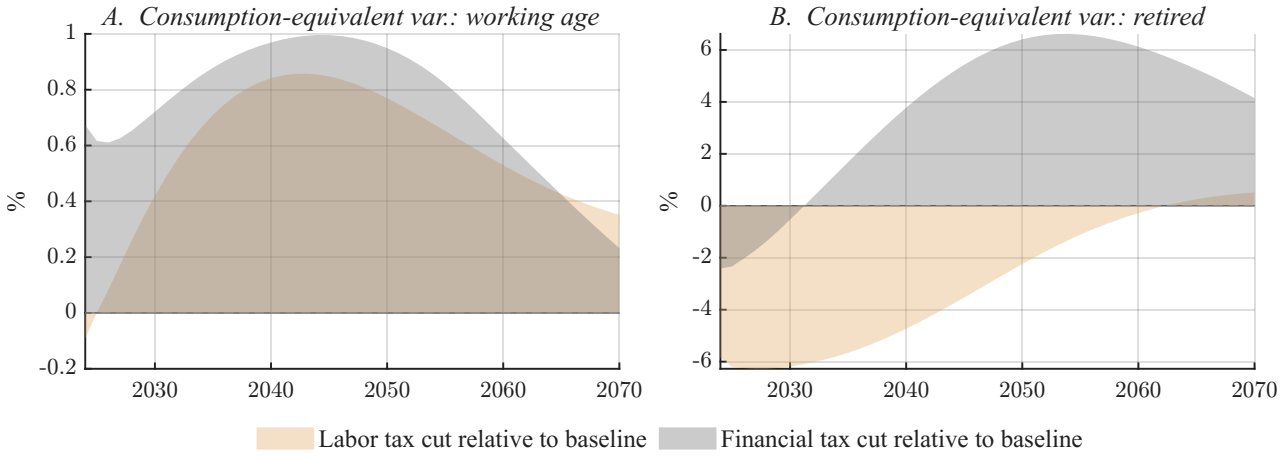


Notes: The panels show the difference (Δ) between the path of a variable (consumption, labor income and financial income) obtained under a given revenue recycling scheme and that obtained under the baseline. The first row (Panels A–C) displays the results for the working age population (aged 20–64) and the second row (Panels D–E) for the retired (aged 65–100). The baseline corresponds to the *Paris-Agreement* scenario, in which carbon revenue is redistributed to households through lump sum transfers.

financial wealth and supports capital accumulation. The resulting capital deepening leads to a stronger and more persistent support to investment and output relative to the baseline (Figure 9), consistent with the fiscal-interaction mechanism of Barrage (2020). On the income side, financial income rises relative to baseline, with gains that are highly concentrated among older and wealthier cohorts, who hold the bulk of financial assets. Working-age households benefit less, as their portfolios are smaller and a larger share of their income derives from labor (Figure 10). This asymmetry is reflected in welfare outcomes. As shown in Figure 11, retired cohorts experience sustained and sizeable welfare gains (up to 6%), while working-age households experience smaller gains (up to 1%), reflecting their lower exposure to the financial-wealth channel. The financial tax cut thus supports aggregate activity while compensating retirees, highlighting a pronounced equity–efficiency trade-off driven by the concentration of financial wealth across cohorts.

Finally, to assess the distributional implications of alternative recycling schemes, we also track the evolution of consumption inequality along the transition path. Panel F of Figure 9 reports the Gini coefficient of the cross-sectional consumption distribution (computed across all living cohorts at each date, weighted by cohort size), providing a summary measure of

FIGURE 11. Intergenerational welfare effects of carbon revenue recycling

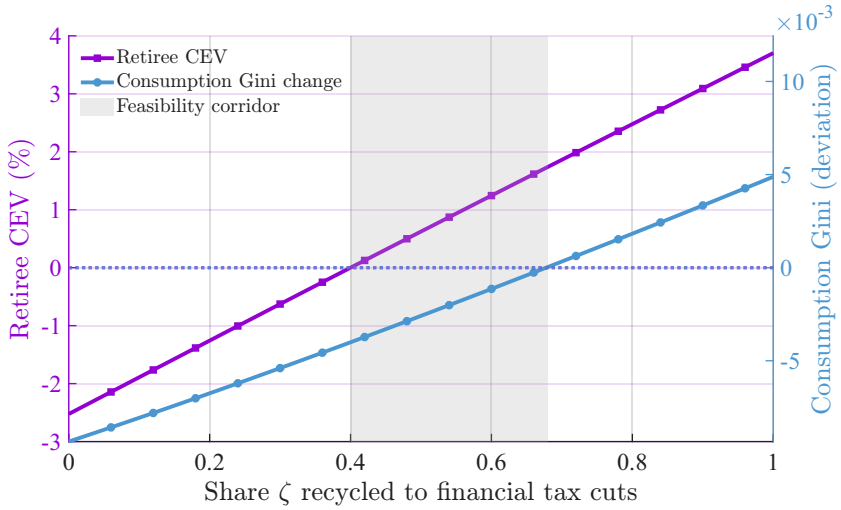


Notes: The panels show the welfare gap between a given revenue recycling scheme and the baseline. Results are reported separately for the working-age population (aged 20–64) and the retired (aged 65–100). The baseline corresponds to the *Paris-Agreement* scenario, in which carbon revenue is redistributed to households through lump sum transfers.

cross-sectional consumption inequality across living cohorts. The labor tax cut compresses the Gini coefficient relative to baseline throughout the transition. By supporting after-tax labor income, it mitigates the income losses borne by working-age households and reduces dispersion in consumption across cohorts. By contrast, the financial tax cut generates a persistent increase in consumption inequality. By raising after-tax returns on assets held disproportionately by older and wealthier households, it amplifies differences in consumption between asset-rich retirees and labor-dependent households. This divergence in the Gini coefficient across recycling schemes quantifies the equity cost of the efficiency gains documented in Panels A–C of Figure 9: the stronger support to output and investment under financial tax cuts comes at the price of a substantially more unequal consumption distribution.

6.2. **Balancing equity and retiree welfare.** The previous subsection shows that no single tax instrument can simultaneously deliver intergenerational compensation and limit inequality. We now examine whether combining labor and financial tax cuts can reconcile these objectives. To this end, we consider revenue-neutral recycling schemes indexed by the share $\zeta \in [0, 1]$ of carbon revenues allocated to financial income tax cuts, with the remaining share devoted to labor tax reductions. Varying ζ therefore allows us to trace a continuum of policy mixes between the two polar cases analyzed above. Equations below formalize how these

FIGURE 12. Carbon tax revenue recycling:
The feasibility corridor for financial tax cuts



Notes: The figure shows the retiree CEV and the change in the consumption Gini relative to the baseline, as a function of the share ζ recycled to financial tax cuts. The shaded region identifies the feasibility corridor over which retirees gain and consumption inequality does not rise.

tax instruments adjust as a function of ζ:

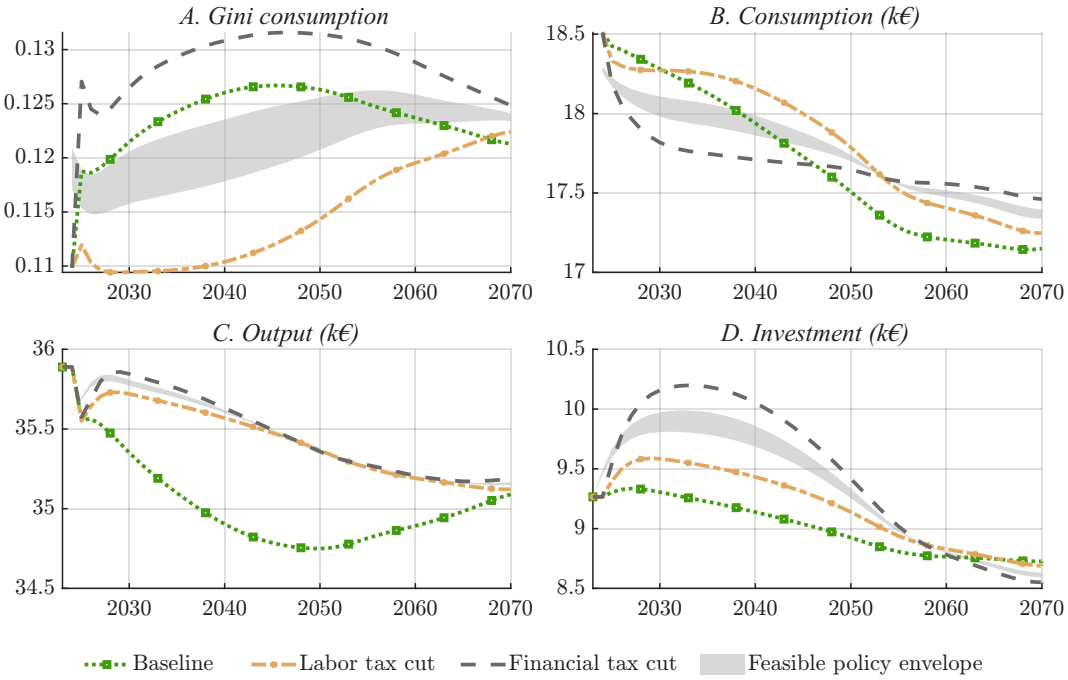
$$(\tau_a - \tau_{a,t})(R_t^a - 1)P_{t-1}a_t = \zeta\tau_{e,t}e_t, \tag{42}$$

$$(\tau_w - \tau_{w,t})W_t h_t = (1-\zeta)\tau_{e,t}e_t. \tag{43}$$

We vary ζ over the unit interval and, for each value, simulate the full transition dynamics of the model. To characterize the feasible policy corridor, we impose two conditions: recycling schemes must deliver non-negative welfare gains for retired cohorts and must not increase consumption inequality relative to the baseline. The corridor is thus defined as the subset of $\zeta \in [0,1]$ for which both conditions hold simultaneously.

Figure 12 reports the consumption-equivalent variation of retired cohorts and the consumption Gini as functions of ζ, both expressed relative to the baseline scenario without double-dividend recycling. A clear trade-off emerges. Increasing ζ raises the CEV of retired cohorts by strengthening the financial-wealth channel, but at the cost of higher consumption inequality. Conversely, lower values of ζ compress inequality but fail to fully compensate retirees. This trade-off implies the existence of a bounded feasible interval. The lower bound is determined by the requirement that retired cohorts experience non-negative CEV, which requires a sufficiently large share of revenues to be allocated to financial tax cuts. The upper bound is pinned down by the inequality constraint, as higher values of ζ disproportionately

FIGURE 13. Carbon revenue recycling schemes and feasible redistribution space



Notes: The figure displays transition paths under the *Paris-Agreement* scenario for three carbon revenue recycling schemes: baseline (lump-sum transfers), labor income tax cut, and financial income tax cut, together with a feasible policy envelope. The envelope (grey area) spans all recycling share parameters $\zeta \in [0.40, 0.68]$ that simultaneously satisfy two distributional constraints: non-negative welfare gains for retired cohorts and a weakly declining Gini coefficient of consumption relative to the baseline.

benefit asset-rich households and increase the dispersion of consumption. Quantitatively, the feasible interval is quite narrow. Retiree CEV becomes non-negative at around $\zeta = 0.40$, while the inequality constraint binds at approximately $\zeta = 0.68$, leaving only a limited range of values that simultaneously satisfy both conditions.

Figure 13 also illustrates the implications of the feasible policy set for transition dynamics over the 2025–2070 horizon. The shaded area reports the range of paths consistent with $\zeta \in [0.40, 0.68]$. Relative to the baseline, feasible recycling schemes sustain higher levels of output and investment throughout the transition, reflecting the partial reallocation of revenues toward financial tax cuts. In terms of consumption, the feasible envelope lies above the financial tax cut case but remains below the baseline in the short run, up to around 2045. This reflects the need to temper the financial-wealth channel to satisfy the distributional constraints, which limits the initial support to aggregate consumption. Over time, however, consumption recovers and eventually exceeds the baseline, as higher capital accumulation translates into stronger income dynamics. Importantly, the feasible envelope lies between the two polar cases. Compared to labor tax cuts, feasible policies deliver stronger support

to capital accumulation and output. Compared to financial tax cuts, feasible policies limit the rise in consumption inequality by tempering the concentration of gains among asset-rich households. These results confirm that the feasible policy space does not eliminate the equity–efficiency trade-off, but rather delineates a region where it remains manageable.[13]

6.3. **Robustness of the feasibility corridor.** The feasibility result established above rests on specific assumptions about nominal rigidities, the pace of the carbon price trajectory, and demographic structure. We assess robustness across six alternative specifications. In each case, we replicate the feasible corridor of Figure 12 under the same two distributional constraints: non-negative CEV for retirees and no rise in the consumption Gini relative to baseline. Figure 14 displays the results.

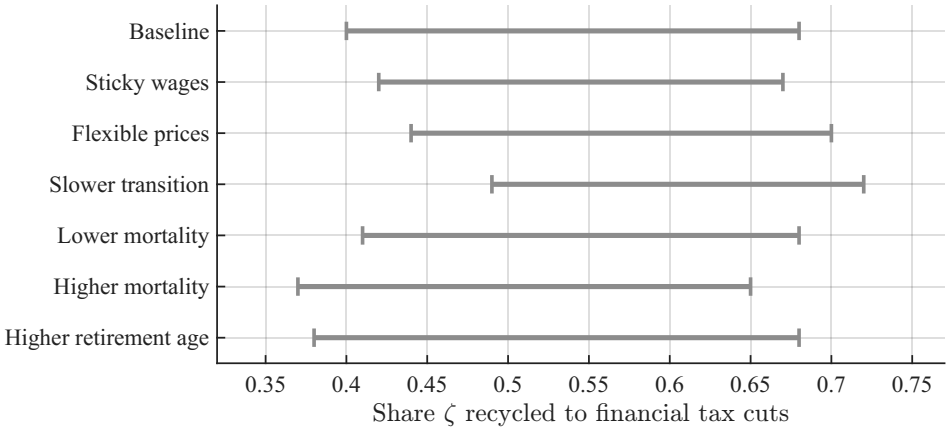
Nominal rigidities. In the first experiment, we introduce sticky wages. Each household is assigned a differentiated labor type, aggregated through a constant-elasticity-of-substitution aggregator. This gives rise to a wage Phillips curve with Rotemberg-style adjustment costs, consistent with the baseline price-rigidity specification $\frac{\kappa_w}{2}\left(\frac{W_t}{W_{t-1}(1+g_{Z,t})}\pi_t - \pi\right)^2 H_t$. The parameter κ_w is calibrated to match the slope of the wage Phillips curve to that of the price Phillips curve, imposing symmetrical nominal rigidity on both margins. Under sticky wages, the lower bound rises to approximately 0.42 while the upper bound remains near 0.67, narrowing the corridor slightly. The additional nominal friction dampens the financial-wealth channel by compressing the real return to assets, requiring a slightly larger share of revenues directed toward capital-income relief to compensate retirees, while tighter wage dynamics limit the scope for labor-tax recycling to reduce inequality.

In the second experiment, we remove price stickiness entirely, setting $\kappa_p = 0$. Under flexible prices, the real allocation is decoupled from monetary policy, and the inflation response to the carbon shock is fully front-loaded rather than spread across the transition. The corridor shifts to approximately $[0.44, 0.70]$, widening at the upper bound relative to baseline. With no price stickiness, the disinflation effect on asset values is more pronounced on impact but dissipates faster, relaxing the inequality constraint at higher values of ζ.

Transition speed. In the third experiment, we replace the *Paris-Agreement* carbon price trajectory with the socially optimal path from Barrage and Nordhaus (2024) at a pure rate of time preference of $\rho = 2\%$. The lower social cost of carbon implies a more gradual ramp-up, smaller fiscal revenues, and a reshaped scope for recycling instruments. The interval shifts

[13] Appendix E shows that, if the policymaker sets its policy on the basis of welfare outcomes for retirees and workers neglecting equity considerations, then the feasibility interval widens to the right up to $\zeta = 1$.

FIGURE 14. Robustness of the feasibility corridor across model variants



Notes: Each bar displays the feasible corridor $[\zeta_{\min}, \zeta_{\max}]$ for a given model specification, where ζ is the share of carbon revenues recycled through financial income tax cuts. The feasible corridor is defined as the set of ζ values satisfying two distributional constraints simultaneously: non-negative consumption-equivalent welfare gains for retired cohorts, and no increase in the consumption Gini relative to the baseline.

rightward, with the lower bound rising to roughly 0.49 and the upper bound extending to nearly 0.72. The more gradual ramp-up generates smaller absolute fiscal revenues: delivering non-negative CEV for retirees therefore requires a larger proportional share directed toward financial tax cuts, shifting $\zeta_{\min}$ upward. At the same time, more diffuse consumption dispersion along the transition relaxes the inequality constraint, pushing $\zeta_{\max}$ outward.

Demographic structure. The fourth experiment perturbs the mortality schedule used to calibrate cohort survival probabilities. Under lower mortality, calibrated to United Nations World Population Prospects for 2033, the corridor shifts marginally relative to baseline, narrowing to approximately $[0.41, 0.68]$: a larger working-age cohort amplifies the labor-income channel, making the inequality constraint bind more tightly and raising $\zeta_{\min}$, while the smaller retiree share limits the redistribution required through financial tax cuts, pulling $\zeta_{\max}$ inward. Under higher mortality, calibrated to realized mortality rates for 2003, the retiree share is larger, the financial-wealth channel more consequential, and the corridor shifts leftward to $[0.37, 0.65]$: a smaller revenue requirement per capita suffices to achieve non-negative retiree CEV at lower values of ζ, pulling both bounds down relative to baseline.

Retirement age. In the final experiment, we raise the mandatory retirement threshold from 64 to 65, reallocating a marginal cohort from retirement to employment along the transition. The corridor shifts to approximately $[0.38, 0.68]$, with the lower bound falling slightly below baseline while the upper bound remains unchanged. The one-year extension of the working life enlarges the pool of near-retirement workers, reducing the per-capita revenue requirement

needed to achieve non-negative retiree CEV and allowing a smaller share directed toward financial tax cuts to suffice, pulling $\zeta_{\min}$ modestly downward.

The corridor found in Section 6 survives across all six specifications. A strictly positive revenue share must flow to financial income tax cuts in every case; the lower bound never falls below 0.37 and the upper bound never exceeds 0.72. Transition speed and demographic structure are the primary determinants of corridor width; nominal rigidities play a secondary role.

7. Monetary policy and the financial-wealth channel: A neutrality result

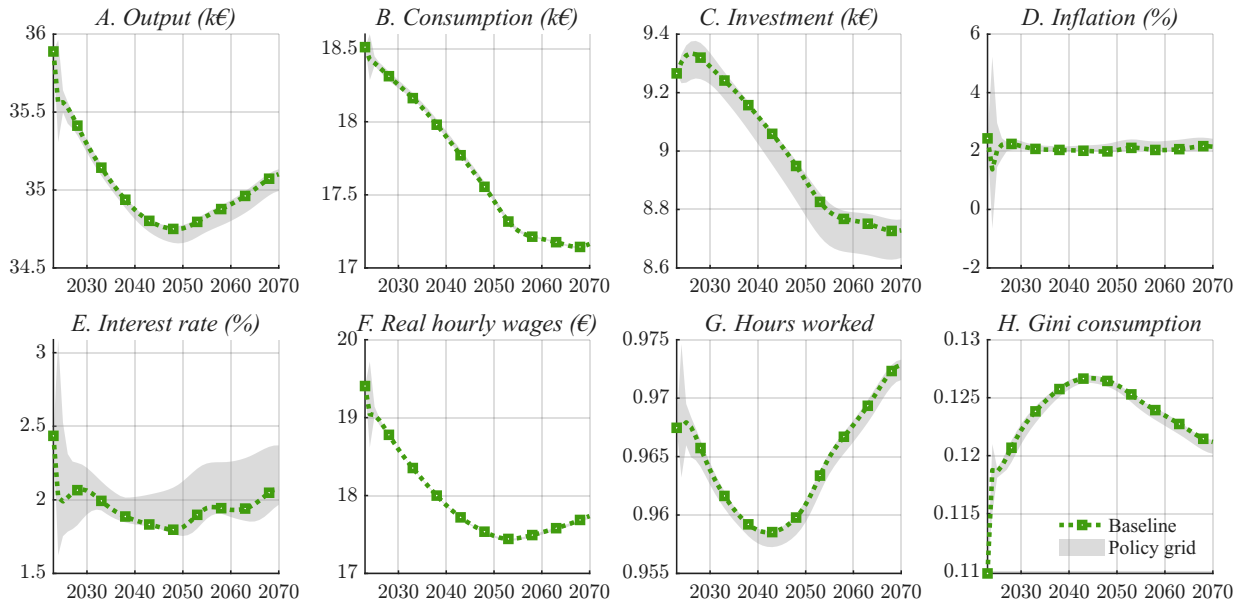
The financial-wealth channel identified in Section 4 has a natural monetary dimension. During the transition, carbon pricing induces a period of disinflation. This raises the real value of nominal asset holdings and the return on financial wealth, generating a transfer toward older households, who are disproportionately exposed to financial income. A more aggressive monetary response could, in principle, dampen this effect by stabilizing inflation and limiting the initial revaluation of nominal assets. This section evaluates whether monetary policy can mitigate the resulting intergenerational redistribution.

7.1. **Sensitivity to monetary policy rules.** We first examine whether alternative monetary policy rules affect the transition dynamics. Figure 15 reports equilibrium paths for a grid of Taylor-rule coefficients, with $\varphi_\pi \in [1.35, 5]$ and $\varphi_y \in [0, 1]$, and compares the resulting envelope with the baseline. The dispersion across rules is small for all main aggregates, including output, consumption, inflation, and inequality. Monetary policy therefore has only limited leverage over the aggregate dynamics of the transition: changing the inflation response mainly affects the timing of price adjustment, without generating sizable differences in real allocations or distributional outcomes.[14]

This limited role reflects two complementary factors. First, carbon pricing operates primarily through real forces: changes in production costs and factor returns. Nominal rigidities shape the short-run adjustment, but they do not drive the main redistributive effects. Second, the OLG structure weakens the standard intertemporal substitution channel. Because survival probabilities decline with age, households have shorter effective planning horizons, which dampens their consumption response to interest-rate changes. Together with borrowing constraints and portfolio adjustment costs, this attenuates the transmission from policy

[14]This conclusion applies to the class of Taylor rules considered here. Under Ramsey-optimal monetary policy, the central bank could in principle exploit nominal rigidities more aggressively to influence real allocations. Solving for the Ramsey allocation, however, is computationally infeasible given the size of the model.

FIGURE 15. Baseline transition and monetary policy grid



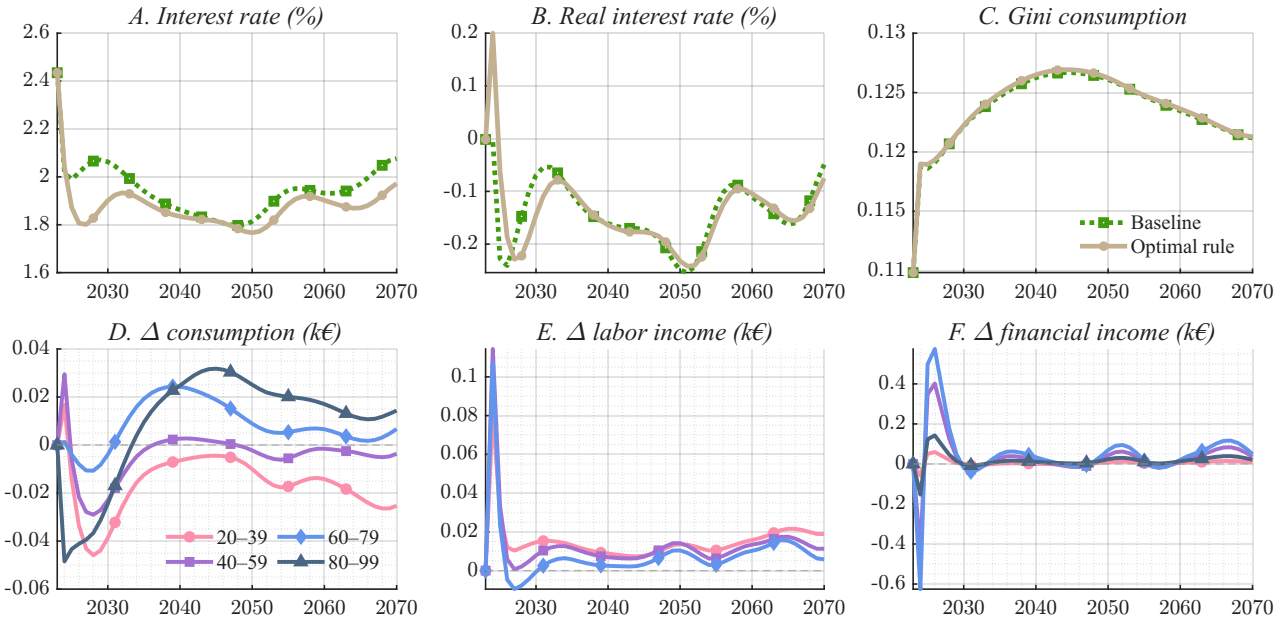
Notes: The figure displays macroeconomic transition paths under the baseline Taylor rule ($\varphi_\pi = 1.925$, $\varphi_y = 0.706$, dotted green line) alongside the policy grid envelope (grey area), which spans all simulated monetary rules over the parameter space $\varphi_\pi \in [1.35, 5]$ and $\varphi_y \in [0, 1]$. The shaded area represents the range of outcomes across the grid of alternative rules.

rates to saving, labor supply, wages, and ultimately labor income. As a result, monetary policy leaves the real redistribution generated by the green transition essentially unchanged.

7.2. **Optimal monetary policy.** We next consider the strongest possible case for monetary intervention by allowing the central bank to optimally choose the parameters of the policy rule to maximize aggregate welfare along the transition path. The optimal rule features a stronger response to inflation and no response to output growth ($\varphi_\pi = 2.65$, $\varphi_y = 0$). Figure 16 compares the transition dynamics under the optimal rule with those obtained under the baseline specification. Despite the more aggressive response to inflation, the resulting allocation remains close to the baseline. Aggregate quantities, inflation dynamics, and inequality therefore exhibit only minor deviations across the two regimes. The lower panels confirm this result at the cohort level. Differences in consumption, labor income, and financial income are concentrated in the first period of the transition and dissipate rapidly thereafter, remaining quantitatively negligible for all age groups beyond the initial adjustment. Even under the welfare-maximizing rule, monetary policy leaves the redistribution force largely unaffected.

These findings imply that monetary policy cannot meaningfully alter the distributional consequences of the transition. Even under an optimal policy rule, the intergenerational redistribution remains largely intact. This contrasts with fiscal policy, which can directly target

FIGURE 16. Baseline versus optimal monetary policy during the transition



Notes: The upper panels display the transition dynamics under the baseline Taylor rule ($\varphi_\pi = 1.925$, $\varphi_y = 0.706$) and under the optimal (welfare-maximizing) monetary policy rule ($\varphi_\pi = 2.65$, $\varphi_y = 0$). The lower panels display the difference in consumption, labor income, and financial income between the two rules for each household cohort.

the underlying sources of redistribution by modifying after-tax income and asset returns. As a result, fiscal instruments, rather than monetary policy, are the primary tool for addressing the distributional effects of carbon pricing.

8. CONCLUSION

This paper studies the intergenerational distributional consequences of the green transition in an overlapping-generations New Keynesian framework. We show that climate policy generates a systematic redistribution across cohorts through two distinct channels: a labor-income channel, driven by wage compression, and a financial-wealth channel, driven by capital gains on nominal assets and higher real returns on financial wealth.

Our analysis delivers three main findings. First, the labor-income channel dominates quantitatively, reflecting the high labor share and the strong exposure of working-age households to wage dynamics. As a result, the transition imposes substantial short-run welfare losses on younger and middle-aged cohorts, while older cohorts benefit from both capital gains and higher financial returns. Second, fiscal policy plays a central role in shaping these outcomes. While carbon revenue recycling can mitigate intergenerational asymmetries, the set of admissible policies is bounded: no single recycling scheme simultaneously satisfies both the

retiree compensation and the inequality constraints, pointing to a genuine equity–efficiency trade-off. Third, monetary policy has limited ability to affect these dynamics. This reflects two complementary factors: carbon pricing operates through real forces rather than nominal rigidities, and the OLG structure attenuates the standard intertemporal substitution channel through shorter effective planning horizons. Monetary policy therefore primarily reshapes the timing of nominal price adjustment without materially altering the real allocation or distributional dynamics across cohorts. Extensions that incorporate credit-market frictions or heterogeneous firm financing, channels through which monetary policy could in principle generate real distributional effects, remain an avenue for future research.

These findings have direct implications for the design of climate policy. The distributional consequences of the transition are not incidental, but arise from fundamental features of the economic structure. Policy design must therefore explicitly account for intergenerational heterogeneity, and revenue recycling emerges as the primary instrument to reconcile political feasibility with distributional objectives. More broadly, our framework highlights the importance of life-cycle structure in shaping the macroeconomic effects of structural transitions, an insight that extends naturally to other contexts involving persistent factor-price realignments.

References

Annicchiarico B, Clipal R, Sahuc JG. 2025. Intergenerational household finance and the green transition cost. *EconomiX Working Paper #2025-30*, University Paris–Nanterre.

Annicchiarico B, Di Dio F. 2015. Environmental policy and macroeconomic dynamics in a New Keynesian model. *Journal of Environmental Economics and Management* **69**: 1–21.

Auclert A. 2019. Monetary policy and the redistribution channel. *American Economic Review* **109**: 2333–2367.

Bachas PJ, Fisher-Post M, Jensen A, Zucman G. 2024. Globalization and factor income taxation. *Working Paper #29819*, National Bureau of Economic Research.

Barrage L. 2020. Optimal dynamic carbon taxes in a climate-economy model with distortionary fiscal policy. *Review of Economic Studies* **87**: 1–39.

Barrage L, Nordhaus W. 2024. Policies, projections, and the social cost of carbon: Results from the DICE-2023 model. *Proceedings of the National Academy of Sciences* **121**: e2312030121.

Baumol WJ, Oates WE. 1988. *The theory of environmental policy*. Cambridge University Press.

Benmir G, Roman J. 2022. The distributional costs of net-zero: A HANK perspective. *Work. Pap., Lond. Sch. Econ. Political Sci., London* .

Bielecki M, Brzoza-Brzezina M, Kolasa M. 2022. Intergenerational redistributive effects of monetary policy. *Journal of the European Economic Association* **20**: 549–580.

Bielecki M, Brzoza-Brzezina M, Kolasa M. 2023. Demographics, monetary policy, and the zero lower bound. *Journal of Money, Credit and Banking* **55**: 1857–1887.

Bovenberg AL, Heijdra BJ. 1998. Environmental tax policy and intergenerational distribution. *Journal of Public Economics* **67**: 1–24.

Christelis D, Georgarakos D, Jappelli T, Pistaferri L, Van Rooij M. 2019. Asymmetric consumption effects of transitory income shocks. *The Economic Journal* **129**: 2322–2341.

Christopoulou R, Vermeulen P. 2012. Markups in the Euro area and the US over the period 1981–2004: A comparison of 50 sectors. *Empirical Economics* **42**: 53–77.

Dietz S, Van Der Ploeg F, Rezai A, Venmans F. 2021. Are economists getting climate dynamics right and does it matter? *Journal of the Association of Environmental and Resource Economists* **8**: 895–921.

Douenne T, Hummel AJ, Pedroni M. 2026. Optimal fiscal policy in a climate-economy model with heterogeneous households. *The Economic Journal* : ueag006.

Druant M, Fabiani S, Kezdi G, Lamo A, Martins F, Sabbatini R. 2012. Firms' price and wage adjustment in europe: Survey evidence on nominal stickiness. *Labour Economics* **19**: 772–782.

European Central Bank. 2006. Estimates of the euro area capital stock. *Monthly Bulletin Boxes* **5**.

European Central Bank. 2024. ECB Statistical Data Warehouse. https://sdw.ecb.europa.eu. Accessed: 2024.

Fagan G, Henry J, Mestre R. 2005. An area-wide model for the euro area. *Economic Modelling* **22**: 39–59.

Fried S, Novan K, Peterman W. 2024. Understanding the inequality and welfare impacts of carbon tax policies. *Journal of the Association of Environmental and Resource Economists* **11**: 231–260.

Gautier E, Conflitti C, Faber RP, Fabo B, Fadejeva L, Jouvanceau V, Menz JO, Messner T, Petroulas P, Roldan-Blanco P, et al. 2024. New facts on consumer price rigidity in the euro area. *American Economic Journal: Macroeconomics* **16**: 386–431.

Golosov M, Hassler J, Krusell P, Tsyvinski A. 2014. Optimal taxes on fossil fuel in general equilibrium. *Econometrica* **82**: 41–88.

Goulder LH. 1995. Environmental taxation and the double dividend: A reader's guide. *International tax and public finance* **2**: 157–183.

Heutel G. 2012. How should environmental policy respond to business cycles? Optimal policy under persistent productivity shocks. *Review of Economic Dynamics* **15**: 244–264.

HFCN. 2023. Household Finance and Consumption Survey: Methodological Report for the 2021 Wave. *Statistical Paper Series #45*, European Central Bank.

Huggett M. 1996. Wealth distribution in life-cycle economies. *Journal of Monetary Economics* **38**: 469–494.

John A, Pecchenino R. 1994. An overlapping generations model of growth and the environment. *The Economic Journal* **104**: 1393–1410.

Jondeau E, Levieuge G, Sahuc JG, Vermandel G. 2026. Environmental subsidies to mitigate net-zero transition costs. *American Economic Journal: Macroeconomics* **Forthcoming**.

Kaplan G, Violante GL. 2014. A model of the consumption response to fiscal stimulus payments. *Econometrica* **82**: 1199–1239.

Karp L, Rezai A. 2014. The political economy of environmental policy with overlapping generations. *International Economic Review* **55**: 711–733.

Keen B, Wang Y. 2007. What is a realistic value for price adjustment costs in New Keynesian models? *Applied Economics Letters* **14**: 789–793.

Kotlikoff L, Kubler F, Polbin A, Sachs J, Scheidegger S. 2021. Making carbon taxation a generational win win. *International Economic Review* **62**: 3–46.

Kotlikoff L, Kubler F, Polbin A, Scheidegger S. 2024. Can today's and tomorrow's world uniformly gain from carbon taxation? *European Economic Review* **168**.

Kouvavas O, Osbat C, Reinelt T, Vansteenkiste I. 2021. Markups and inflation cyclicality in the euro area. *Working Paper #2617*, European Central Bank.

Kuhn M, Schlattmann L. 2024. Distributional consequences of climate policies. *Discussion Paper #18893*, Centre for Economic Policy Research.

Lis E, Nickel C, Papetti A. 2020. Demographics and inflation in the euro area: A two-sector New Keynesian perspective. Working Paper #*2382*, European Central Bank.

McAdam P, Willman A. 2013. Medium run redux. *Macroeconomic Dynamics* **17**: 695–727.

Mouabbi S, Sahuc JG. 2019. Evaluating the macroeconomic effects of the ECB's unconventional monetary policies. *Journal of Money, Credit and Banking* **51**: 831–858.

OECD. 2025. Taxing Wages 2025: Decomposition of Personal Income Taxes and the Role of Tax Reliefs. Technical report, OECD Publishing.

Rezai A, van der Ploeg F. 2026. Carbon pricing incidence in an overlapping generations economy. *Discussion Paper #21246*, Centre for Economic Policy Research.

Sahuc JG, Smets F, Vermandel G. 2024. The New Keynesian climate model. *Working paper #977*, Banque de France.

Smets F, Wouters R. 2003. An estimated dynamic stochastic general equilibrium model of the euro area. *Journal of the European Economic Association* **1**: 1123–1175.

Smets F, Wouters R. 2007. Shocks and frictions in US business cycles: A Bayesian DSGE approach. *American Economic Review* **97**: 586–606.

United Nations. 2024. World Population Prospects 2024. Online Edition, United Nations,Department of Economic and Social Affairs, Population Division.

ONLINE APPENDIX

–NOT INTENDED FOR PUBLICATION–

TABLE OF CONTENTS

Appendix A Equilibrium conditions of the model 42
Appendix B HFCS aggregation procedure 45
Appendix C Age-profile of labor income as a share of total income 46
Appendix D Age profile of consumption-equivalent welfare costs 47
Appendix E A welfare-based feasibility criterion 49

APPENDIX A. EQUILIBRIUM CONDITIONS OF THE MODEL

This appendix presents the equilibrium conditions of the model. All the aggregates are now expressed in efficiency units, and we use a tilde to denote such variables. The relative carbon price is defined as $\tilde{\tau}_{e,t} = \tau_{e,t}/P_t$, the real rental rate of capital is given by $r_t^k = R_t^k/P_t$, while the price of a unit of capital expressed in real terms is $q_t = Q_t/P_t$. We define mc_t as the real marginal cost of production for intermediate-goods producers, gross of environment-related costs (abatement and policy), while the term $\varpi_t > 0$ denotes the component of the marginal cost associated with the manufacturing process. We define the Lagrange multiplier on the no-borrowing constraint (the Kuhn-Tucker multiplier) of households as $\tilde{\lambda}_{j,t}^a$. Finally, we denote by g public spending as a share of output.

Demographics.

- $N_t = \sum_{j=1}^{J} N_{j,t}$
- $N_t = (1+n)N_{t-1}$
- $N_j^{rel} = N_{j,t}/N_t$, for $j \in [1:J]$
- $N_j^{rel} = \frac{1-\omega_{j-1}}{1+n} N_{j-1}^{rel}$, for $j \in [2:J]$

Household sector.

- $(1+g_{z,t+1})\,\tilde{a}_{j+1,t+1} = \tilde{x}_{j,t} + \frac{1}{\pi_t}[1+(1-\tau_{a,t})(R_t^a-1)]\tilde{a}_{j,t} - \frac{\kappa_a}{2}\tilde{x}_{j,t}^2$, for $j \in [1:(J-1)]$
- $\tilde{x}_{j,t} = (1-\tau_{h,t})\tilde{w}_t z_j h_{j,t} + \widetilde{beq}_t + \tilde{\tau}_{j,t} - \tilde{c}_{j,t}$ for $j \in [1:(JR-1)]$

- $\tilde{x}_{j,t} = \widetilde{beq}_t + \tilde{\tau}_{j,t} - \tilde{c}_{j,t}$
  for $j \in [JR : J]$
- $\tilde{a}_{1,t} = 0$
- $\tilde{a}_{J+1,t+1} = 0$
- $\varphi_j h_{j,t}^{\nu} = \frac{z_{j,t}\tilde{w}_t(1-\tau_{h,t})}{\tilde{c}_{j,t}}$, for $j \in [1 : (JR-1)]$
- $h_{j,t} = 0$, for $j \in [JR : J]$
- $1 = \beta(1-\omega_j)\mathbb{E}_t\left\{\frac{\tilde{c}_{j,t}}{(1+g_{z,t+1})\tilde{c}_{j+1,t+1}}\frac{1+(1-\tau_{a,t+1})(R_{t+1}^a-1)}{\pi_{t+1}}\frac{1-\kappa_a\tilde{x}_{j,t}}{1-\kappa_a\tilde{x}_{j,t+1}}\right\} + \tilde{\lambda}_{j,t}^a$, for $j \in [1 : (J-1)]$
- $\tilde{a}_{j+1,t+1} \geq 0$, $\tilde{\lambda}_{j,t}^a \geq 0$ and $\tilde{\lambda}_{j,t}^a \tilde{a}_{j+1,t+1} = 0$, for $j \in [1 : (J-1)]$

Aggregation.

- $\tilde{c}_t = \sum_{j=1}^{J} N_j^{rel}\tilde{c}_{j,t}$
- $h_t = \sum_{j=1}^{JR-1} \frac{N_j^{rel} z_j h_{j,t}}{N^{rel}}$
- $\tilde{a}_{t+1} = \sum_{j=1}^{J-1} \frac{N_j^{rel}}{1+n}\tilde{a}_{j+1,t+1}$
- $\widetilde{beq}_t = \sum_{j=2}^{J} \frac{\omega_{j-1}N_{j-1}^{rel}}{1+n}\frac{1+(1-\tau_{a,t})(R_t^a-1)\tilde{a}_{j,t}}{\pi_t}$
- $\tilde{\tau}_t = \sum_{j=1}^{J} N_j^{rel}\tilde{\tau}_{j,t}$

Financial sector.

- $(1+n)(1+g_{z,t+1})\tilde{k}_{t+1} = (1-\delta)\tilde{k}_t + \left[1 - \frac{\kappa_i}{2}\left(\frac{\tilde{\imath}_t}{\tilde{\imath}_{t-1}} - 1\right)^2\right]\tilde{\imath}_t$
- $1 = q_t\left[1 - \frac{\kappa_i}{2}\left(\frac{\tilde{\imath}_t}{\tilde{\imath}_{t-1}} - 1\right)^2 - \kappa_i\left(\frac{\tilde{\imath}_t}{\tilde{\imath}_{t-1}} - 1\right)\frac{\tilde{\imath}_t}{\tilde{\imath}_{t-1}}\right] +$
  $+\mathbb{E}_t\left\{q_{t+1}\frac{\pi_{t+1}}{R_t}\kappa_i\left(\frac{\tilde{\imath}_{t+1}}{\tilde{\imath}_t} - 1\right)\left(\frac{\tilde{\imath}_{t+1}}{\tilde{\imath}_t}\right)^2(1+n)(1+g_{z,t+1})\right\}$
- $\mathbb{E}_t\left\{\pi_{t+1}\left[u_{t+1}r_{t+1}^k + (1-\delta)q_{t+1}\right]\right\} = R_t q_t$
- $r_t^k = r^k \exp\left(\frac{\psi_k}{1-\psi_k}(u_t - 1)\right)$
- $\tilde{a}_{t+1} - \tilde{b}_{t+1} = \left[q_t(1-\delta)\tilde{k}_t + \tilde{\imath}_t\right] / \left[(1+n)(1+g_{z,t+1})\right]$
- $\frac{R_t^a}{\pi_t}\tilde{a}_t - \frac{R_{t-1}}{\pi_t}\tilde{b}_t = \left[u_t r_t^k + (1-\delta)q_t\right]\tilde{k}_t + \tilde{d}_t - \frac{1-\psi_k}{\psi_k}r^k\left[\exp\left(\frac{\psi_k}{1-\psi_k}(u_t-1)\right) - 1\right]\tilde{k}_t$

Business sector.

- $\tilde{y}_t = (1 - \mathcal{D}(T_t))\left(u_t\tilde{k}_t\right)^{\alpha} h_t^{1-\alpha}$
- $mc_t = \sigma_t\tilde{\tau}_{e,t}(1-\mu_t) + \phi_{1,t}\mu_t^{\phi_2} + \varpi_t$
- $\tilde{w}_t = (1-\alpha)\varpi_t\frac{\tilde{y}_t}{h_t}$
- $r_t^k = \alpha\varpi_t\frac{\tilde{y}_t}{\tilde{k}_t}$

- $\tilde{d}_t = \left(1 - mc_t - \frac{\kappa_p}{2}\left(\pi_t - \pi\right)^2\right)\tilde{y}_t$
- $\tilde{\tau}_{e,t} = \frac{\phi_{1,t}\phi_2\mu_t^{\phi_2-1}}{\sigma_t}$
- $\tilde{e}_t = \sigma_t\left(1-\mu_t\right)\tilde{y}_t$
- $1 - \frac{\varepsilon_p}{\varepsilon_p - 1} + mc_t\frac{\varepsilon_p}{\varepsilon_p - 1} - \kappa_p\left(\pi_t - \pi\right)\pi_t + \frac{\kappa_p}{R_t}\mathbb{E}_t\left\{\left(\pi_{t+1} - \pi\right)\pi_{t+1}^2\frac{\tilde{y}_{t+1}(1+g_{Z,t+1})}{\tilde{y}_t}\right\}$

Public sector.

- $\tilde{g}_t = g\tilde{y}_t$
- $\left(1+n\right)\left(1+g_{z,t+1}\right)\tilde{b}_{t+1}^g = \frac{R_{t-1}}{\pi_t}\tilde{b}_t^g + \tilde{g}_t - \bar{\tau}_{e,t}\tilde{e}_t + \tilde{\tau}_t - \left[\tau_{a,t}(R_t^a - 1)\right]\frac{\tilde{a}_t}{\pi_t} - \tau_{h,t}\tilde{w}_t h_t$
- $\frac{R_t}{R} = \left(\frac{R_{t-1}}{R}\right)^{\varphi_r}\left[\left(\frac{\pi_t}{\pi}\right)^{\varphi_\pi}\left(\frac{\tilde{y}_t}{\tilde{y}_{t-1}}\right)^{\varphi_y}\right]^{(1-\varphi_r)}$

Market clearing and pollution.

- $\tilde{b}_t = \tilde{b}_t^g$
- $\tilde{y}_t = \tilde{c}_t + \tilde{\imath}_t + \tilde{g}_t + \phi_{1,t}\mu_t^{\phi_2}\tilde{y}_t + \frac{\kappa_p}{2}\left(\pi_t - \pi\right)^2\tilde{y}_t + \frac{1-\psi_k}{\psi_k}r^k\left[\exp\left(\frac{\psi_k}{1-\psi_k}\left(u_t - 1\right)\right) - 1\right]\tilde{k}_t + \frac{\kappa_x}{2}\tilde{x}_{j,t}^2$
- $\mathcal{D}(T_t) = \gamma_1 T_t + \gamma_2 T_t^2$
- $T_t = T_{t-1} + \xi_T\bar{E}_t^{tot}$
- $E_t = Z_t N_t\tilde{e}_t = \sigma_t\left(1-\mu_t\right)Z_t N_t\tilde{y}_t$

Trends.

- $Z_t = \left(1+g_{z,t}\right)Z_{t-1}$
- $g_{z,t} = g_{z,t-1}(1-\delta_z)$
- $\phi_{1,t} = \phi_{1,t-1}(1-\delta_\phi)$
- $\sigma_t = \sigma_{t-1}(1-\delta_\sigma)$

Rest of the world.

- $E_t^* = E_t^{tot} - E_t$

APPENDIX B. HFCS AGGREGATION PROCEDURE

This appendix describes the step-by-step aggregation procedure applied to each wave of the Household Finance and Consumption Survey.

In each wave, we aggregate HFCS microdata by age in six steps. First, missing values in financial variables are set to zero so that all households enter the sample regardless of asset or income category. Second, all variables are divided by the square root of household size (DH0001) to obtain individual-equivalent quantities. Third, we exploit the multiple-imputation structure of the HFCS: for each combination of age (DHAGEH1), country (SA0100), and implicate (IM0100), we compute weighted means using the household survey weights, then average across the five implicates to obtain point estimates. Fourth, we construct the variables of interest described in the main text. Fifth, monetary amounts are deflated using the harmonized index of consumer prices for the euro area (see Table B.1), expressing all quantities in constant 2021 euros. Sixth, we renormalize age-group weights to match the actual age distribution in the euro area, computed from the HFCS age variable (RA0300), so that the final euro-area aggregates reflect the true demographic composition rather than the sample composition.

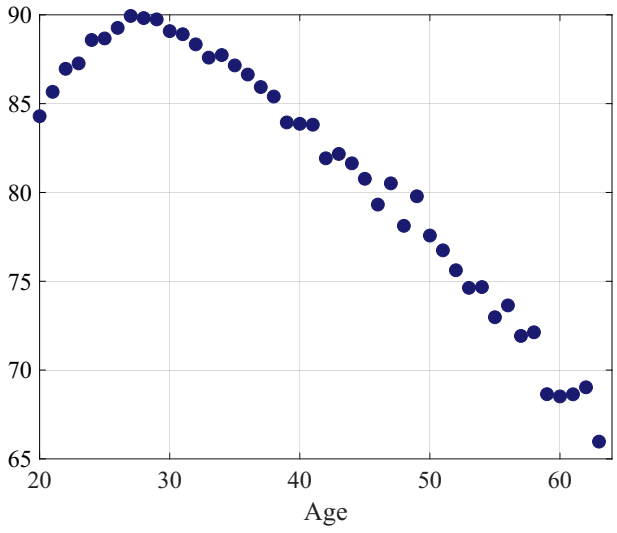
TABLE B.1. Inflation adjustment factors *(relative to 2021 euros)*

	2010	2014	2017	2021
Belgium	1.2131	1.1241	1.0738	1.0000
Germany	1.1780	1.0997	1.0695	1.0000
Estonia		1.1534	1.0980	1.0000
Ireland		1.0150	1.0040	1.0000
Greece	1.0732	1.0063	0.9981	1.0000
Spain	1.0719	1.0326	1.0218	1.0000
France	1.1649	1.0778	1.0612	1.0000
Croatia			1.0237	1.0000
Italy	1.1123	1.0310	1.0310	1.0000
Cyprus	1.0718	1.0034	1.0248	1.0000
Latvia		1.0885	1.0546	1.0000
Lithuania			1.1497	1.0000
Luxembourg	1.1987	1.0968	1.0518	1.0000
Malta	1.1588	1.0845	1.0542	1.0000
Netherlands	1.2059	1.1057	1.0846	1.0000
Austria	1.2365	1.1236	1.0798	1.0000
Portugal	1.1265	1.0439	1.0135	1.0000
Slovenia	1.1397	1.0615	1.0549	1.0000
Slovakia	1.2164	1.1114	1.1054	1.0000
Finland	1.1597	1.0467	1.0318	1.0000

APPENDIX C. AGE PROFILE OF LABOR INCOME AS A SHARE OF TOTAL INCOME

Figure C.1 reports the share of labor income in total income across working-age cohorts, from age 20 to retirement at age 64, computed from the calibrated model at the pre-transition steady state. From age 28 onward, the share declines monotonically with age, reflecting the rising contribution of financial income over the working life. For the very young workers, the share initially rises with age: younger workers enter the labor market with lower remuneration (as shown in Figure 1), so their labor income contributes less to total resources at the very start of working life. The figure complements the results of Section 5 by showing that exposure to the negative effects of the transition operating through the labor-income channel is itself strongly heterogeneous across generations.

FIGURE C.1. Age profile of labor income as a share of total income (%)



Notes: The figure reports the age profile of labor income as a share of total income for working-age cohorts in the model's pre-transition steady state. The vertical axis measures shares in %. The horizontal axis reports working ages.

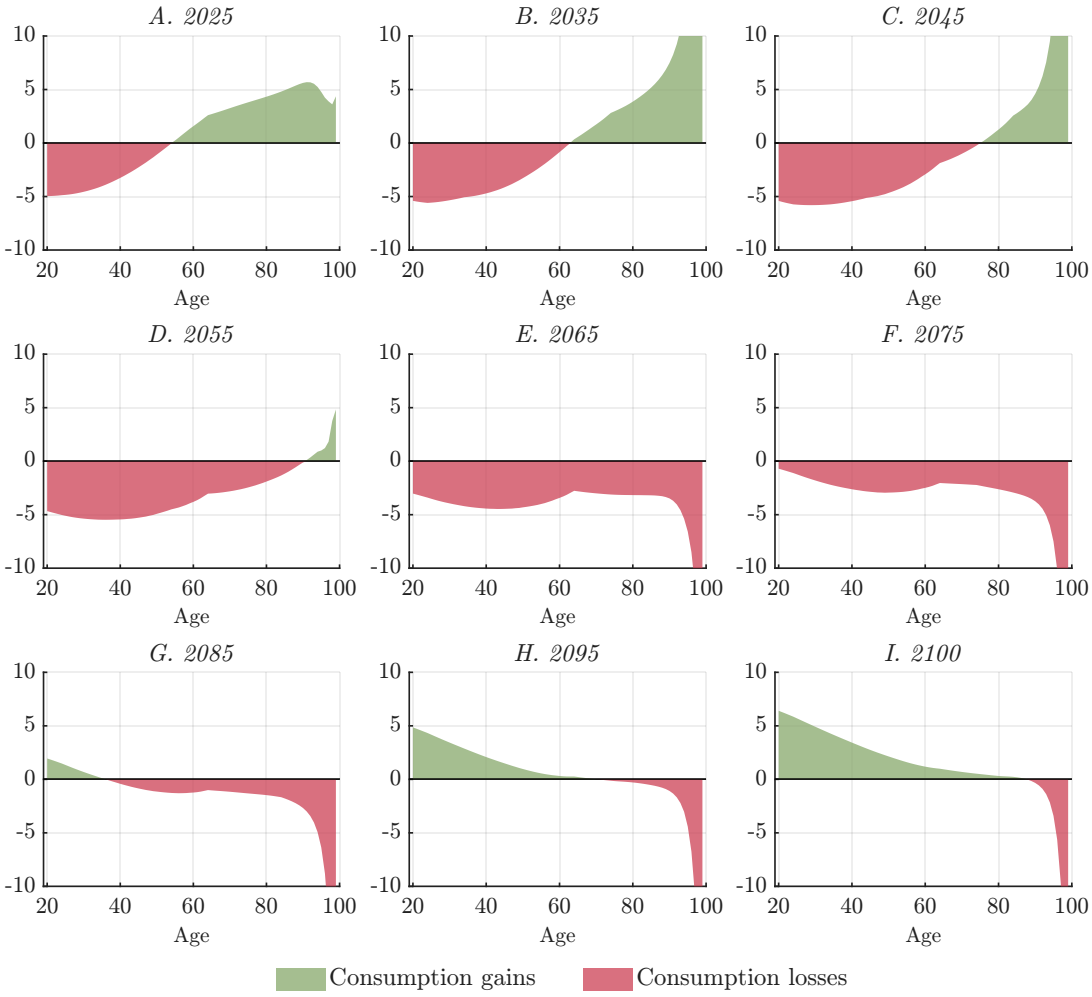
APPENDIX D. AGE PROFILE OF CONSUMPTION-EQUIVALENT WELFARE COSTS

Figure D.1 complements the cohort-level analysis of Figure 8 by plotting the full age distribution of $\Im_{j,t}$ at nine successive dates along the transition path. Reading across panels, two regularities emerge. First, the early decades of the transition (Panels A through C, 2025–2045) exhibit a pronounced age gradient: households aged 80 and above record consumption gains that exceed 20 percent at the top of the distribution (the vertical axis is truncated at 10 percent to preserve readability across panels), reflecting the financial-wealth channel through which asset-rich older cohorts benefit from the capital reallocation triggered by the *Paris Agreement*, while working-age cohorts face losses of 4–6 percent concentrated among the youngest households.

Second, this age gradient flattens and then inverts over time. By mid-century (panels D–E, 2055–2065), the green area has almost entirely vanished: welfare gains across the distribution have vanished, consistent with the progressive depletion of asset positions that sustained the financial-wealth channel benefit in earlier decades, so that losses now extend across virtually the entire age distribution. This is the cross-sectional counterpart of the convergence observed in Figure 8, where all four cohort trajectories cluster around their joint welfare trough near 2065.

In the final three decades (Panels G–I, 2085–2100), the distribution rotates again as the long-run climate dividend materialises: younger cohorts progressively move into positive territory while the sharp losses concentrate among the very old, who bear residual transition costs without benefiting from the avoided climate damages accruing over the remainder of the century. Together, the nine panels underscore that the intergenerational redistribution induced by the green transition is not a static transfer but a dynamic process whose direction and magnitude shift substantially as the transition unfolds.

FIGURE D.1. Age profile of welfare costs along the transition path

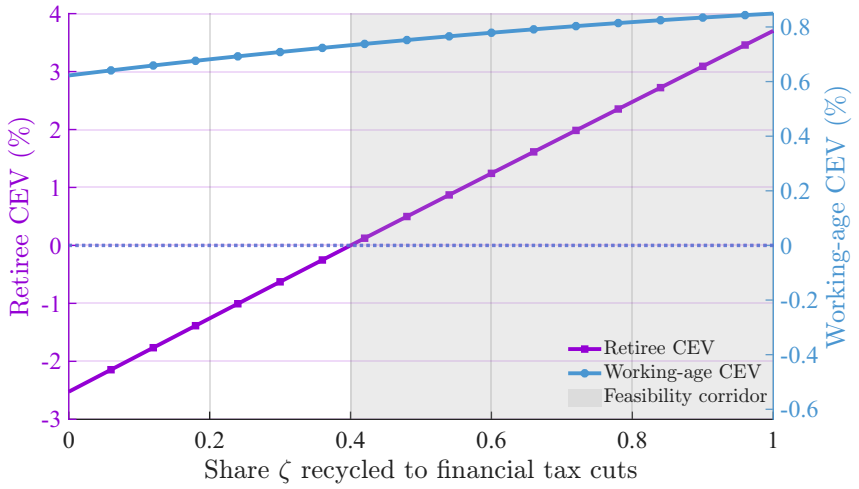


Notes: Each panel reports the consumption-equivalent variation $\Im_{j,t}$ across cohorts aged 20–100 at several dates along the transition path. $\Im_{j,t}$ is the proportional shift in the *Low Carbon Price* baseline consumption stream required to match lifetime utility under the *Paris Agreement*. The vertical axis measures the magnitude of the consumption-equivalent variation in percent of baseline consumption, where red (resp. green) shading indicates a loss (resp. gain) of consumption relative to the *Paris Agreement*. The horizontal axis reflects the age distribution of living cohorts at each date.

APPENDIX E. A WELFARE-BASED FEASIBILITY CRITERION

The feasibility corridor defined in Section 6 combines two distributional constraints: non-negative welfare gains for retired cohorts and a weakly declining consumption Gini relative to baseline. The Gini criterion captures the concern for intergenerational inequality, but one may ask what the feasible policy space would look like if the policymaker focused exclusively on welfare outcomes, that is, if the feasibility criterion required non-negative welfare gains for both retired *and* working-age cohorts simultaneously, without imposing any constraint on the consumption distribution.

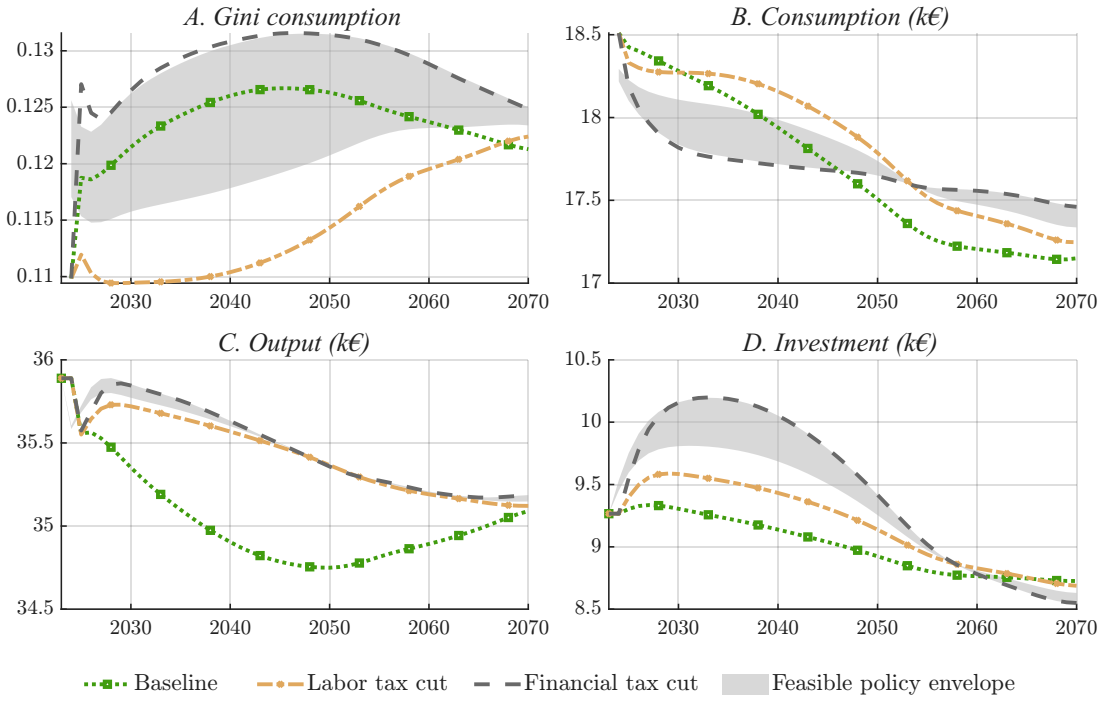
FIGURE E.1. Feasibility corridor based on retiree and working-age welfare gains



Notes: The figure shows the retiree consumption-equivalent variation (CEV) and the working-age CEV as a function of the share ζ recycled to financial tax cuts. The shaded region identifies the feasibility corridor over which both cohorts gain.

Figures E.1 and E.2 report the results under this alternative criterion. The feasible interval widens to $\zeta \in [0.40, 1]$: since working-age welfare improves monotonically with ζ, financial tax cuts stimulate asset returns and relax intertemporal budget constraints, any recycling share that compensates retirees is also compatible with working-age welfare gains. The absence of a Gini constraint therefore removes the upper bound on the feasibility zone. This comparison illustrates that the tightness of the feasible interval identified in the main text is driven by the equity constraint rather than by the welfare constraint: redistributing too aggressively toward financial tax cuts can simultaneously benefit all cohorts in welfare terms while widening the consumption distribution.

FIGURE E.2. Carbon revenue recycling schemes: feasible corridor under retiree and working-age welfare gains



Notes: The figure displays transition paths under the *Paris-Agreement* scenario for three carbon revenue recycling schemes: baseline (lump-sum transfers), labor income tax cut, and financial income tax cut, together with a feasible policy envelope. The envelope (grey area) spans all recycling share parameters $\zeta \in [0.40, 1]$ that simultaneously satisfy non-negative welfare gains for both retired and working-age cohorts.